UNIVERSIDADE DO ALGARVE

Role of Chemerin and its receptors in mouse models of tumorigenesis

Bárbara Sofia Marques da Silva

Dissertação de Mestrado em Oncobiologia – Mecanismos Moleculares do Cancro

Trabalho efetuado sob a orientação de:

Marc Parmentier (IRIBHM, University Free of Brussels, Belgium)

Virginie Robert-Gavioli (IRIBHM, University Free of Brussels, Belgium)

Ana Teresa Maia (Universidade do Algarve, Portugal)

2015

UNIVERSIDADE DO ALGARVE

Role of Chemerin and its receptors in mouse models of tumorigenesis

Bárbara Sofia Marques da Silva

Dissertação de Mestrado em Oncobiologia – Mecanismos Moleculares do Cancro

Trabalho efetuado sob a orientação de:

Marc Parmentier (IRIBHM, University Free of Brussels, Belgium)

Virginie Robert-Gavioli (IRIBHM, University Free of Brussels, Belgium)

Ana Teresa Maia (Universidade do Algarve, Portugal)

2015

Role of Chemerin and its receptors in mouse models of tumorigenesis

Declaro ser a autora deste trabalho que é original e inédito. Autores e trabalhos consultados estão devidamente citados no texto e constam da listagem de referências incluída.

_____

(Barbara Silva)

Agradecimentos

Em primeiro lugar, gostaria de agradecer pela ótima oportunidade que o Professor Marc Parmentier me deu ao aceitar-me *no Institut de Recherche Interdisciplinaire de Biologie Humaine et Moleculaire (IRIBHM), Université Libre de Bruxelles*, Bélgica, permitindo-me assim fazer parte desta equipa e deste projecto.

A Virginie Robert-Gavioli por todo o tempo dispensado a ensinar-me tanto, pelo seu conhecimento, a sua paciência e apoio ao longo deste ultimo ano.

A toda a equipa do professor Marc Parmentier pela sua ajuda, apoio e bom humor, em particular a Maxime Vernimmen e Mustapha Chaouni por me ajudarem na manipulação de experiências e pelo manuseamento dos ratinhos.

A todos os Professores do Mestrado em Oncobiologia – Mecanismos Moleculares do Cancro, Departamento de Ciências Biomédicas e Medicina, Universidade do Algarve, pelo apoio, conhecimento e conselhos dados ao longo destes últimos dois anos.

Aos amigos que me apoiaram incondicionalmente neste ano difícil e nunca duvidaram das minhas capacidades.

E por todo o amor, apoio, afeto e paciência dada pelas pessoas mais importantes do mundo, os meus pais e a minha irmã, porque sem eles, nada seria possível, nem o mais pequeno teste, nem o maior dos desafios.

Acknowledgements

First, I would like to thank the optimal opportunity that Professor Marc Parmentier gave me by accepting me into IRIBHM and permit me to be part of this team and this project.

To Virginie Robert-Gavioli for all the time she spent teaching me so much, for her knowledge, her patience and for her support throughout this year.

To the whole Parmentier's Team for their help, support and good humor, in particular to Maxime Vernimmen and Mustapha Chaouni for helping me in several experiments and the management of mice.

To all the Professors at the Master in Oncobiology - Molecular Mechanisms of Cancer, Department of Biomedical Sciences and Medicine, University of Algarve, for their support, knowledge and advice given along these two years.

To some friends who have supported me unconditionally in this difficult year and never doubted my abilities.

And for all the love, support, affection and patience given by the most important people, my parents and my sister. Because without them, nothing would be possible, even the smallest test or the greatest of challenges.

Abstract

Chemerin is a chemoattractant factor for leukocytes involved in various inflammatory diseases and human cancers. This protein is acting through three G protein-coupled receptors: ChemR23, GPR1 and CCRL2.

ChemR23 is the main receptor, present in immune cells and non-immune cells. Its main function is described as involving the migration of various leukocyte populations. GPR1 is expressed mainly in the central nervous system. It binds chemerin with high affinity but signals poorly, and its functional role is presently unclear. CCRL2 is a non-functional receptor expressed by immune cells and endothelial cells. Its proposed role is to concentrate chemerin and present the ligand to ChemR23-expressing cells.

In this work, we intended to contribute to the understanding of the role of CCRL2 and ChemR23 in tumor development using, for each receptor, genetically deficient mouse lines and tumor cell line grafts. Using B16 melanoma and Lewis lung carcinoma cell lines as models, we did not observe differences in tumor growth and recruitment of leukocyte populations to the experimental tumors in ChemR23-deficient mice, suggesting that ChemR23 does not affect the tumor development.

In the CCRL2 absence, we observed a significant decrease of tumor growth, suggesting a pro-tumoral effect of CCRL2. The immune cell recruitment and the blood chemerin levels were similar in CCRL2-deficient and wild-type mice. The proliferative and apoptotic cells were analyzed by fluorescence microscopy, in tumors from wild-type and CCRL2-deficient mice. The tumor cells proliferated equally in the two groups. However, we observed a higher proportion of apoptotic cells and necrotic areas in the absence of CCRL2. As CCRL2 is present in endothelial cells, we tested whether the increase of apoptotic cells could be explained by an alteration of angiogenesis in the absence of the receptor. We analyzed for this purpose the expression of factors known to regulate angiogenesis in tumors from $CCRL2^{+/+}$ and $CCRL2^{-/-}$ mice. The results showed that CCRL2

invalidation affects the expression of thrombospondin 1 (TSP1), vascular endothelial growth factor A (VEGFA) and fibroblast growth factor 2 (FGF2).

Although further experiments will be necessary to confirm and extent our observations, we have shown in this work that CCRL2 contributes to tumor angiogenesis and support therefore tumor progression, preventing necrosis and apoptosis of tumor cells.

Key-words

Chemerin; CCRL2; ChemR23; angiogenesis; apoptosis; cancer

Resumo

A chemerin foi identificada no nosso laboratório como sendo uma proteína quimioatraente de células imunitárias. Vários estudos mostraram que esta proteína pode apresentar um efeito inibitório ou promotor de tumores, dependendo do tipo de cancro. Se por um lado, foi mostrado um efeito anti-tumoral em cancros do pulmão, próstata e melanoma, onde a concentração de chemerin está diminuída em pacientes doentes, outro estudo mostra um aumento de chemerin em pacientes com diferentes tipos de cancros gástricos, e por isso, apresenta um efeito pro-tumoral.

A chemerin é encodada pelo gene *tazarotene-induced 2*, e é expressa principalmente no fígado e tecido adiposo, mas também na glândula adrenal, pâncreas, pulmões e pele. O seu precursor, prochemerin, está biologicamente inativo e requer uma clivagem proteolítica para se ativar e tornar-se chemerin.

A chemerin tem a capacidade de se ligar a três receptores acoplados a proteína G: ChemR23, GPR1 e CCRL2.

ChemR23 é descrito como o principal receptor da chemerin e é expresso em células do sistema imunitário como macrófagos e células *natural killer*, mas também em células não hematopoiéticas, como adipócitos e células endoteliais. A ligação da chemerin ao receptor ChemR23 promove a internalização do receptor, a mobilização de cálcio e a quimiotaxia de células imunitárias que expressam este receptor. Alguns estudos mostraram funções do sistema chemerin/ChemR23 a nível inflamatório, que pode influenciar a migração das células endoteliais, apresentando um efeito anti-inflamatório.

GPR1 é expresso em células do sistema nervoso, placenta, pele, entre outros, mas não em células do sistema imunitário. Este receptor liga-se com elevada afinidade a chemerin, ocorrendo a internalização do receptor. Porém, não foi detetada nenhuma sinalização intracelular. Desta forma, a função deste receptor e a sua interação com a chemerin continua por esclarecer.

CCRL2 encontra-se presente em macrófagos, células dendríticas e em células endoteliais. Este receptor liga-se com elevada afinidade a chemerin, mas não ocorre sinalização intracelular nem a internalização do receptor, sugerindo que este receptor é não funcional. Foi mostrado a hipótese que CCRL2 apresenta a chemerin ao receptor ChemR23, e que tem a capacidade de promover a migração de células dendríticas via a chemerin.

Com este projeto, pretendemos compreender o papel da chemerin e de dois receptores, CCRL2 e ChemR23, no desenvolvimento tumoral. Para tal, usamos ratinhos deficientes para cada um dos receptores que recebem xenógrafos de linhas celulares tumorais. Este modelo de tumorigenése permitirá analisar quais os processos tumorais afetados por estes receptores, tal como, a proliferação e apoptose de células tumorais, o recrutamento de populações de células imunitárias e a expressão de fatores angiogénicos.

Para analisar o efeito da deficiência de ChemR23 no desenvolvimento tumoral, foi injectado um milhão de células provenientes de melanoma (linha B16) nos flancos de ratinhos *wild-type* e knock-out para ChemR23. Os tumores foram medidos diariamente até dez dias após a implantação.

0Os resultados mostram que os tumores em ratinhos *wild-type* e knock-out para ChemR23 surgem de forma igual e que desenvolvem de igual forma. Isto sugere que ChemR23 não está envolvido no desenvolvimento tumoral, neste modelo tumoral. Observamos, igualmente, a influência de ChemR23 na migração de células imunitárias atá ao site tumoral, via citometria de fluxo. Os resultados mostraram que a ausência de ChemR23 não afetou a migração de células imunitárias, no geral, nem as diversas subpopulações analisadas, sugerindo que este receptor não influencia a migração das células imunitárias em resposta a um tumor. Estes resultados são consistentes com os resultados observados no crescimento tumoral.

Para saber se CCRL2 está envolvido no controlo do desenvolvimento tumoral, um milhão de células B16 foram injetadas nos flancos em ratinhos *wild-type e knock-out* para CCRL2, observando o desenvolvimento tumoral ao longo de vários dias. Os tumores dos ratinhos *wild-type* e *knock-out* desenvolvem-se ao mesmo tempo mas nos ratinhos knock-out os tumores são menores. Estes resultados sugerem que CCRL2 tem um efeito pró-tumoral neste modelo tumoral. Este efeito foi confirmado com outra linha de células tumorais provenientes de carcinoma pulmonar de Lewis, que apresentou resultados semelhantes.

Para perceber o efeito de CCRL2 na migração de células imunitárias, analisamos o recrutamento de células imunitárias em tumores de células B16, por citometria de fluxo. As populações de células imunitárias foram analisadas diversos dias após a implantação tumoral (3, 6 e 10 dias). Os resultados das diferentes análises sugerem que tanto a população total de células imunitárias como as diversas subpopulações não são afetadas pela ausência de CCRL2. Estes resultados foram confirmados por microscopia de fluorescência, onde se marcou células imunitárias com anticorpos fluorescentes em cortes de tumores. Os resultados mostraram a mesma proporção de células imunitárias, bem como a mesma distribuição em ambos os grupos de ratinhos. Confirmamos que CCRL2 não afeta o recrutamento de células imunitárias ao realizar a mesma experiência com tumores de células LLC, obtendo assim os mesmos resultados.

De forma a perceber o efeito de CCRL2 no desenvolvimento tumoral e a sua influência na migração de células imunitárias, determinamos as consequências do défice de CCRL2 nas concentrações plasmáticas totais de chemerin. Amostras de sangue de ratinhos *wild-type* e *knock-out* foram analisadas por ELISA. Os resultados mostraram que a concentração nos dois grupos é igual, sugerindo que a concentração total de chemerin não é afetada por este receptor.

Via um teste aequorin e purificação por HPLC (*high pressure liquid chromatography*), foi analisada a concentração plasmática de chemerin bioativa

nos dois grupos de ratinhos, e observou-se que a concentração era similar nos dois grupos.

A concentração total de chemerin também foi analisada, por ELISA, após a implantação de células tumorais. Os resultados mostraram um aumento da concentração de chemerin após a implantação tumoral em ambos os grupos de ratinhos. Porém, não foram observadas diferenças da concentração plasmáticas na ausência de CCRL2.

Estes resultados sugerem que o efeito observado em CCRL2 não pode ser explicado pela concentração de chemerin plasmática total e ativa, visto que esta não é alterada estas experiências mostram que a diminuição de tamanho de tumores em ratinhos knock-outs não se deve a concentração de chemerin nem a proporções de células imunitárias recrutadas para o site tumoral.

Por estar presente em células endoteliais, tentamos perceber a influência de CCRL2 na neo-angiogénese tumoral e as consequências na sobrevivência celular e proliferação tumoral.

A proliferação e a apoptose celular foram analisadas por imunofluorescência, em tumores de células B16, a três e a seis dias de desenvolvimento tumoral. Ao analisar a colocalização de células em proliferação, observamos semelhante proliferação em ratinhos *wild-type* e *knock-out*, nos dois dias, sem aparentarem diferenças, sugerindo que CCRL2 não afeta este processo.

Analisamos a apoptose celular em tumores de células LLC a dez dias de desenvolvimento tumoral, por imunofluorescência. Observamos um aumento de células apoptóticas, na ausência de CCRL2, quando comparado ao grupo *wild-type*. Observamos também que as regiões apoptóticas estão à periferia das regiões necróticas, que também estão aumentadas, comparando com o grupo *wild-type*. Estes resultados mostram que CCRL2 parece ter um efeito nos processos de apoptose e na necrose deste modelo tumoral.

Estes processos estão correlacionados com a angiogénese tumoral. Desta forma, para entender a interação com CCRL2, observou-se a expressão de fatores angiogénicos em tumores de células LLC a dez dias de desenvolvimento tumoral, por PCR quantitativa.

Os resultados mostraram que, na ausência de CCRL2 a expressão de trombospondina-1, VEGFA e FGF2 estão aumentados comparando com o grupo controlo. Estes resultados preliminares sugerem que CCRL2 pode ter uma significante influência no controlo da angiogénese tumoral, moldada pela expressão de fatores angiogénicos, e consequentemente, alterando a apoptose tumoral.

Com este trabalho, é possível concluir que ChemR23, receptor principal da chemerin, não influencia o desenvolvimento tumoral nem o recrutamento imunitário, não estando por isso implicado nos efeitos antitumorais da chemerin, neste modelo tumoral. Por outro lado, CCRL2, um receptor não-funcional, apresenta um efeito pró-tumoral no mesmo modelo experimental. Este efeito deve-se a sua influência na angiogénese, que poderá vir a ser explicado pela sua implicação na expressão de trombospondina-1 ou na migração de células endoteliais.

Como perspetiva, pretendemos compreender melhor o papel de CCRL2 a nível da angiogénese. Com isto, analisaremos a expressão de outros fatores angiogénicos, a correlação com o TSP1, VEGFA e o FGF2, bem como na influência na migração de células endoteliais para o site tumoral.

Palavras-chave:

Chemerin; CCRL2; ChemR23; angiogenése; apoptose; cancro.

Index

Index of tables and figures

Abbreviations

7-AAD: 7-aminoactinomycin

APCs: antigen presenting cells

APC: allophycocyanin

BSA: bovine serum albumin

CCL2: Chemokine (C-C Motif) Ligand 2

CCRL2: C-C Chemokine Receptor Like 2

CMKLR1: chemokine-like receptor 1

ChemR23: chemerin receptor 23

CHO: Chinese hamster ovary

CXCL1: Chemokine (C-X-C Motif) Ligand 1

CXCL2: Chemokine (C-X-C Motif) Ligand 1

Cy: Cyanine

DC: dendritic cells

DNA: deoxyribonucleid acid

EC: endothelial cells

EDTA: Ethylenediamine tetraacetic acid

FBS: fetal bovine serum

FITC: fluorescein isothiocyanate

FGF2: Fibroblast Growth Factor 2

GAPDH: Glyceraldehyde-3-Phosphate Dehydrogenase

GPCR: G protein-coupled receptor

HIF1 alpha: hypoxia induced factor subunit 1 alpha

HPLC: high pressure liquid chromatography

IL1beta: Interleukin 1 beta

IL6: Interleukin 6

IL10: Interleukin 10

LLC: Lewis lung carcinoma

MDSC: myeloid derived supressor cells

MMP7: matrix metalloprotease 7

MMP9: matrix metalloprotease 9

MMP10: matrix metalloprotease 10

NK cells: natural killer cells

Nm: nanomolar

PBS: phosphate buffered saline

pDC: plasmacytoid dendritic cells

PFA: paraformaldehyde

PE: R-phycoerythrin

PerCP: Peridinine Clorophyll Protein Complex

RARRES2: retinoid acid receptor responder protein 2

RT: room temperature

RT-qPCR: reverse transcriptase quantitative polymerase chain reaction

Streptavidin-HRP: streptavidin Horseradish peroxidase

TGF-beta: Transforming Growth Factor, Beta 1

TIG2: tazarotene-induced gene 2

TNFalpha: Tumor necrosis factor alpha

TSP1: thrombospondin 1

VEGFA: Vascular Endothelial Growth Factor A

1. INTRODUCTION

1.1 CANCER

Presently, cancer is a major problem in public health throughout the world, accounting for over a quarter of all deaths in developed countries (Macharet et al., 2015).

In 2012, cancer had an incidence of 14.1 million new cases and killed about 8.2 million patients worldwide. In Portugal, the values are also high, with an incidence of 426 patients for 100,000 individuals, and cancer kills about one third of these patients. Globally, 40% of those cases are due to lung, breast, colorectal and stomach cancers, the most common being lung cancer in men and breast cancer in women (Direção-Geral de Saúde, 2014) (World Cancer Factsheet, 2014).

A malignant tumor is the result of the accumulation of DNA mutations in a cell or in a population of identical cells - a clone - in determinant genes, resulting in the transformation of a normal cell to a tumor cell. These mutations lead to the loss of the normal function of the gene, or rather to its uncontrolled activity, promoting aberrant or uncontrolled cell growth, decreasing apoptotic cell death, enhancing angiogenesis and cell migration and driving ultimately the development of distant metastases (Brennan, 2012).

There are many differences amongst the various types of cancer, but there is a set of common properties that are shared by all types, which are defined as the “hallmarks of cancer”. These hallmarks include sustained proliferative signaling, evasion from growth suppressors, escape from apoptosis, tissue invasion and metastasis, unlimited replicative potential, sustained angiogenesis, evasion of immune surveillance, deregulated cellular energetics, genomic instability, and tumor promoting inflammation (Macharet et al., 2015).

The main characteristic of a tumor cells is their ability to proliferate in an uncontrolled manner. In tumor cells, the signaling pathways leading to proliferation are often activated constitutively, while the cells have gained the ability to escape from the effects of proliferative suppressors, such as TGF-β. This supports a permanent and excessive proliferation, resulting in genomic instability in the cell, thereby increasing the number of acquired mutations and, consequently, accelerating the tumor progression. In combination with excessive cell proliferation, there is also an excessive cell growth, due to the ability of tumor cells to escape growth suppressors, such as p53 and the retinoblastoma protein (pRb). The cancer cells also gain a high capacity to resist cell death by evasion from apoptotic inducers and the upregulation of telomerase, which makes them immortal (Broertjes, 2015).

The immune system has been viewed as a promising target for anticancer therapy, as it has the potential to recognize cancer cells and kill them through the activation of various effector pathways. However, several studies have shown that inflammation plays a dual role in tumor development. Immune cells, through chronic inflammation, have the ability to produce molecules that promote tumor cell proliferation, resistance to cell death, angiogenesis, genetic instability and metastasis. In addition, some cancer cells have also gained the ability to escape from the immune detection system, which represents an obvious selective advantage during tumor progression (Broertjes, 2015).

The uncontrolled proliferation of tumor cell induces a high pressure in the tissue, which prevents the adequate supply of oxygen and nutrients to tumor cells. In response to hypoxic conditions that result from the relative lack of blood supply, the cells change their metabolic program, favoring aerobic glycolysis over oxidative phosphorylation, and leading to an energetic dysregulation in the cell. To counteract the state of hypoxia, tumor cells induce the production of new blood vessels irrigating the tumor, by secreting angiogenic factors such as VEGF and FGFs (Broertjes, 2015).

The vascularization of a tumor also allows the tumor cells to metastasize. The metastatic process begins by an invasion of surrounding tissue by the tumor cells, followed by the intravasation of cells into the bloodstream and / or the lymphatic vessels following their passage through the endothelial wall, and finally the extravasation of cancer cells to a distant tissue or organ away from the primary tumor. The biggest challenge for metastatic tumor cells is survive in the new microenvironment they face at the metastatic sites (Broertjes, 2015).

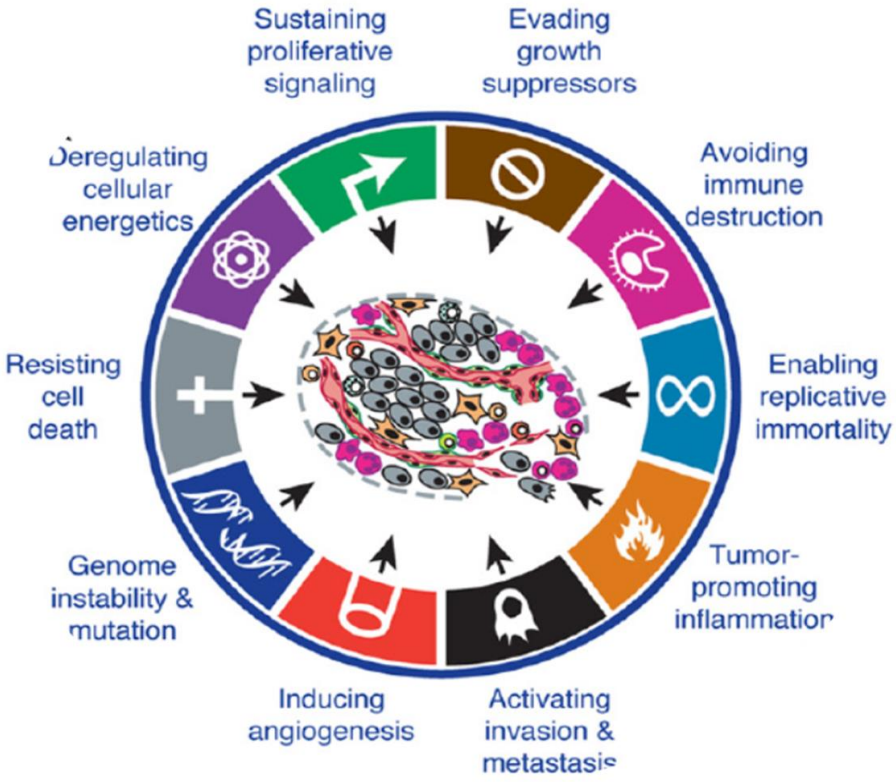

Figure 1.1 Hallmarks of cancer. *To become tumoral, a normal cell is the target of several molecular events, which result in sustained proliferative signaling, evasion of growth suppressors, escape from apoptosis, tissue invasion and metastasis, etc. (Adapted from Hanahan et al., 2011)*

The susceptibility to developing cancer results from genetic and epigenetic factors as well as environmental factors such as exposure to external carcinogens.

Genetic factors can be inherited for a small fraction. The frequency of genetically inherited cancers is indeed relatively low. Most genetic alterations are somatic and accumulate in cells during development and thereafter. Genes that are frequently mutated in cancer can be divided in two groups: the proto-oncogenes, where the mutations activate the gene product and thereby contributes to the tumor development; and suppressor tumor genes, in which the mutations inhibit the gene function, thereby affecting its antitumoral properties such as induction of apoptosis and inhibition of proliferation. Some of the most common mutations found in human tumors affect genes such as TP53, PIK3CA3, PTEN, APC, VHL, KRAS, etc. (Macharet et al, 2015).

Epigenetics has also an important role in cancer, because alteration of epigenetics marks can affect the function of DNA segments, independently of its sequence. The epigenetic alterations can occur as changes in DNA methylation, post-translational histone modifications, and in non-coding RNA or interference RNA (RNAi) that control the stability and translation of protein-encoding transcripts (Herceg, 2007).

The external carcinogens can be environmental and divided in three groups: outdoor air pollutants (industrial polluents); indoor air pollutants (tobacco) and pollutants present in water, such as the arsenic (Broffeta et al., 2003). Thus, it is considered that cancer is a complex multifactorial disease (Brennan, 2012).

To better understand the cancer development and plan a potential anticancer treatments, it is necessary to understand the early stages of a tumor and the interactions of the cancer cells with the tumor microenvironment.

1.2 TUMOR MICROENVIRONMENT

Excessive proliferation prevents adequate supply of oxygen and nutrients to the tumor, inducing apoptosis and necrosis.

To grow up and to sustain their excessive proliferation, tumor cells need to interact with their microenvironment and create a milieu favorable to the development of the tumor. This requires the building of an adequate blood supply, but also the control of the immune system, which may otherwise combat tumor cells and lead to their apoptotic or necrotic death.

Tumor angiogenesis consists in the formation of new vessels from preexisting ones, in response to the production of angiogenic factors by tumor cells or the tumoral stroma. The tumor vasculature is characterized to be structurally and functionally chaotic, both in size and shape, with a discontinuous endothelium, extended basement membrane and aberrant pericyte coverage (Horssen et al., 2006) (Stockmann et al., 2014). In the absence of angiogenesis, the growth of primary tumors is limited and metastases remain dormant. When tumoral cells undergo what is called an “angiogenic switch”, they become able to secrete angiogenic factors. These factors promote sprouting from neighboring blood vessels and the migration of endothelial cells toward the tumor (Horssen et al., 2006).

Aberrant cell proliferation also promotes the migration of leukocytes to the tumor site. The primary function of recruited cells from the innate immune system is to stop tumor progression. NK cells are the first immune population to detect tumor cells, and kill them by contact. (Finn, 2012) NK cells have two lytic mechanisms: (1) release of granzymes and perforin; (2) induction of apoptosis through the release of tumor necrosis factor alpha (TNFα). Dendritic cells and macrophages (APC) are resident cells in normal tissues, acting as sentinels probing the microenvironment and responding to stress signals. APCs have the capacity to recognize tumor cells through the detection of antigens resulting from genetic

mutations (Chimal-Ramirez et al., 2013). APCs secrete many inflammatory cytokines in the tumor site and present tumor antigens to T lymphocytes (T cells) and B lymphocytes (B cells) in the draining lymph nodes. APCs induce the clonal expansion of tumor antigen-specific T cells, and activate $CD4^+$ helper and $CD8^+$ cytotoxic T cells. $CD4^+$ helper T cells have the capacity to produce inflammatory cytokines that increase the migration of leukocytes to the tumor site. $CD8^+$ cytotoxic T cells recognize specifically the tumor cells and induce their apoptosis through the release of perforin and granzymes (Quail et al., 2013). APC also present tumor antigens to B cells, activating them. As $CD4^+$ and $CD8^+$ T cells, B cells belong to the adaptive immune system, and they produce specific antibodies to prevent tumor recurrence (Finn, 2012).

Various mechanisms allow tumor cells to escape the immune system. Tumors can indeed recruit and modify the behavior of several immune cell populations, which will display anti-inflammatory functions. It includes myeloid-derived suppressor cells (MDSC), regulatory T cells (Treg) and M2 macrophages. The presence of these cells in the tumor microenvironment will in turn inhibit the host anti-tumoral immune response and promote instead tumor growth and neoangiogenesis. The anti-tumoral activity of $CD4^+$ and $CD8^+$ T cells can be regulated by anti-inflammatory cells such as regulatory T cells (Treg) and myeloid-derived suppressor cells (MDSC). Treg cells have the capacity to produce immunosuppressive cytokines, kill directly conventional T cells, and inhibit the priming of these cells in lymphoid tissues (Gallimor et al., 2008). MDSCs have the ability to inhibit the function of $CD4^+$ and $CD8^+$ T cells by several mechanisms, including the inhibition of T cell proliferation in response to antigenic peptides and the loss of expression of TCR ζ chain (Watanabe et al., 2008). MDSCs also act on NK cells by suppressing their cytotoxic activity by the inhibition of IL2-mediated NK cell activation and the inhibition of perforin production (Liu et al., 2010).

Although macrophages have an anti-tumoral role through their antigen-presenting capability, a subset, the so-called M2 polarized macrophages, promote

instead tumor development. They are able to migrate to the hypoxic regions of tumors and induce angiogenesis, by the secretion of angiogenic factors such as VEGF and FGF2. They promote tumor cell invasion by the secretion of several growth factors, such as IL-10, VEGFA and arginase-1 (Quail et al., 2013).

The immune cells migrate to the tumor site in response to chemoattractant factors. The chemokines and other chemoattractant proteins and lipids are produced by local cells in an injured tissue. These molecules diffuse and produce a concentration gradient allowing leukocyte recruitment. Many chemokines were shown to play a role in in tumor progression, including CXCL1, CXCL2, CXCL8, CCL2 and their receptors CXCR1, CXCR2, CCR2 and CCR5, among others (Allavena et al., 2010) (Zhao et al., 2005). The chemoattractant molecules and their receptors could represent important targets for the development of therapeutic approaches able to control tumor progression.

A new chemoattractant protein for immune cell populations, chemerin, was identified in the host laboratory a decade ago. Several studies have shown the role of chemerin in tumor development, with a pro or anti-tumoral effect, depending on the type of cancer. Pachynski et al. demonstrated that chemerin expression is down-regulated in many human cancers such as melanoma, and that high chemerin expression correlates with a higher recovery rate in melanoma patients (Pachynski et al, 2012). However, Wang et al. showed that patients with gastric cancer (particularly individuals with poor prognosis or with non-intestinal type) have increased chemerin levels (Wang et al., 2014).

1.3 CHEMERIN

The gene encoding chemerin was first described as tazarotene-induced gene 2 (Tig2 or RARRES2). Chemerin is expressed mainly by the liver and adipose tissue, but also by the adrenal gland, pancreas, lung and skin (Zabel et al., 2014). The preprochemerin precursor form (163 amino acids) includes a typical signal peptide of 20 residues, which is cleaved during the import into endoplasmic reticulum. A prochemerin form with 143 amino acids is therefore secreted by cells, and represents the dominant isoform in the plasma of healthy subjects (~3 nM) (Mattern et al., 2014) (Due et al., 2009). Prochemerin is biologically inactive, and requires proteolytic processing at its C-terminus to become active. There are at least eight proteases involved in the cleavage of prochemerin to shorter forms, either active - chemerin - or inactive. These proteases include neutrophil serine proteases (cathepsin G and elastase), tryptase and plasmin (Figure 1.2). Cathepsin G and elastase are responsible to convert prochemerin into two isoforms of bioactive chemerin, which act as potent chemoattractant molecules for leucocyte populations (Mattern et al., 2014).

Chemerin production can be regulated by metabolic or inflammatory mediators, including agonists of nuclear receptor (retinoids, vitamin D, glucocorticoids), factors associated with metabolic processes (fatty acids, insulin, glucose) and immunoregulatory mediators (inflammatory cytokines, LPS) (Zabel et al., 2014). Chemerin is able to bind to three G protein-coupled heptahelical receptors with high affinity: ChemR23, GPR1 and CCRL2.

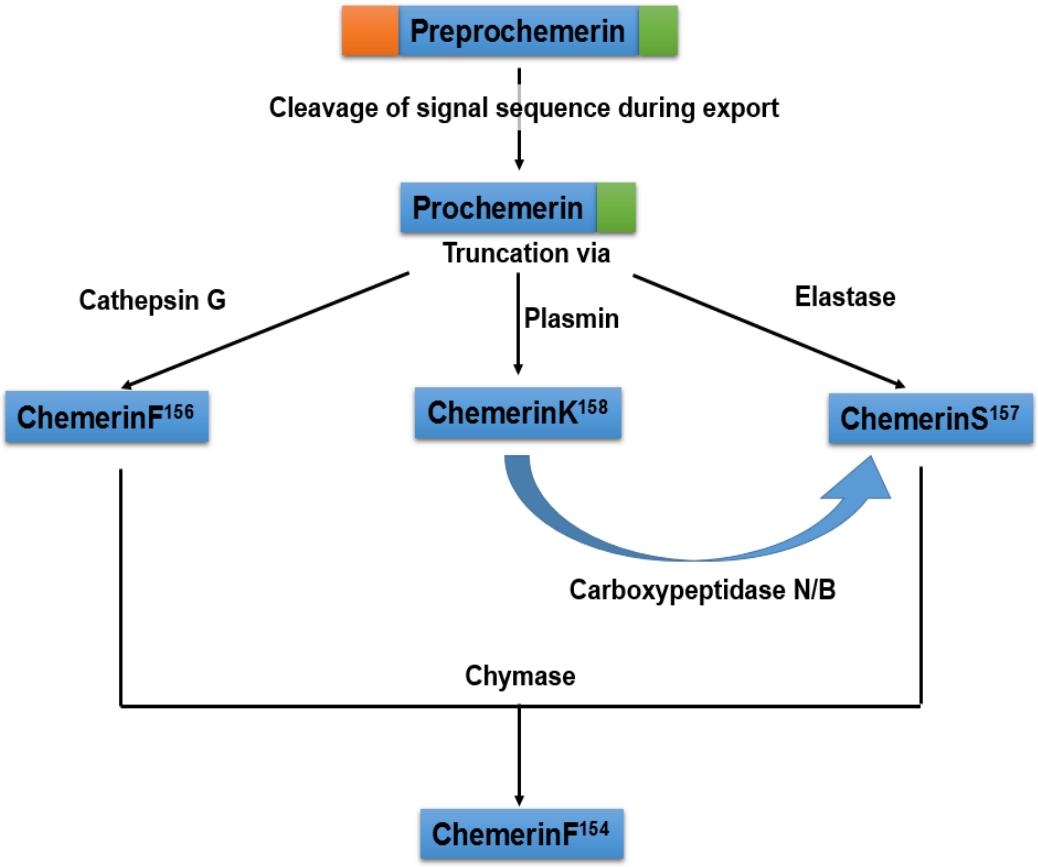

Figure 1.2 Mechanisms of chemerin cleavage. *Chemerin is first produced as preprochemerin, and following the co-translational cleavage of the signal peptide, it becomes prochemerin, the main isoform present in the plasma of healthy subjects. Prochemerin can be truncated in different isoforms, depending of the processing enzymes. The various isoforms have different functions in biological processes such as immune recruitment, angiogenesis or regulation of glucose metabolism (Adapted from Mattern et al., 2014).*

1.3.1. ChemR23

ChemR23, also described as Chemokine-like receptor 1 (CMKLR1) or DEZ in mice, is a G protein-coupled receptor, which was described as the first receptor of chemerin (Wittamer et al., 2003). It was later described to bind also the lipid mediator resolvin E1 (RevE1) (Arita et al., 2007), although the putative interaction between resolvin E1 and ChemR23 is still a matter of debate. ChemR23 is

expressed by immune cells such as monocytes, macrophages, NK cells, and myeloid and plasmacytoid dendritic cells. ChemR23 expression is downregulated during the maturation of dendritic cells. The receptor is also expressed in non-immune cells, including preadipocytes and adipocytes, osteoclasts, chondrocytes, skeletal muscle cells and endothelial cells (Bondue et al., 2012).

GPCRs are composed of seven transmembrane helices, three intracellular loops and three extracellular loops. They signal through trimeric G protein G, composed of αβγ subunits, and a set of effectors (Wu et al., 2012)(Tuteja, 2009). GPCRs are activated by extracellular ligands, promoting the release of GDP from the α subunit of the G protein and its replacement by GTP (Wu et al., 2012) (Tuteja, 2009). The dissociation of G_{α} and $G_{\beta\gamma}$ subunits allow them to bind effectors such as adenylyl cyclase, phospholipase C beta, PI3Ks and ion channels. These effectors regulate in turn various signaling cascades involving intracellular enzymes, transporters and channels and transcription factors (Wu et al., 2012) (Tuteja, 2009).

Binding of chemerin to ChemR23 (K_D = 4.9 nM; EC_{50} = 4.5 nM) promotes internalization of the receptor, calcium mobilization and chemotaxis of ChemR23-expressing immune cells (Bondue et al., 2012) (Herová et al., 2015). In the host laboratory, Luangsay et al. showed an anti-inflammatory effect of the chemerin/ChemR23 system in an animal model of acute lung inflammation. They observed an accumulation of neutrophils in the lung and a high production of proinflammatory cytokines following an intranasal instillation of LPS. When chemerin was given together with LPS, the recruitment of neutrophils and the production of cytokines were milder, indicating an anti-inflammatory role of chemerin. In ChemR23-deficient mice, the recruitment of neutrophils to the lung increased compared to wild-type mice, suggesting that the anti-inflammatory effect of chemerin is mediated by ChemR23 (Luangsay et al., 2009).

1.3.2 GPR1

GPR1 is expressed in the nervous system, placenta, ovary and testis, skin, adipose tissue and skeletal muscle, but not in the immune system (Zabel et al., 2014). GPR1 binds chemerin with high affinity (K_D = 5.3 nM), and internalizes efficiently. However, the signaling elicited by this receptor, which includes Ca^{2+} mobilization and ERK1/2 phosphorylation, is much less efficient than that promoted by ChemR23 (Zabel et al., 2014) (Mattern et al., 2014). The functional role of this receptor in the chemerin system is therefore still unclear. No evidence was provided so far to show cell migration mediated by GPR1. It was suggested that GPR1 could act as a decoy receptor, regulating the chemerin concentration in the plasma by its internalization and its degradation (Zabel et al., 2014).

1.3.3 CCRL2

CCRL2 (C-C Chemokine Receptor Like 2), is described as the third receptor having chemerin as a ligand. CCRL2 is structurally related to the family of chemokine receptors, sharing 40% identity with CCR1, CCR2 and CCR5 (Mattern et al., 2014). The human receptor is expressed by immune cells such as monocytes, macrophages, dendritic cells (DC), neutrophils, T cells, NK cells, mast cells and $CD34^+$ precursors of the bone marrow. In mice, the receptor is expressed by mast cells, macrophages, dendritic cells and endothelial cells (Bondue et al., 2011).

CCRL2 binds chemerin with high affinity both in human and mice (K_D = 1.6 nM). However, the binding of chemerin does not lead to internalization of CCRL2 or Ca^{2+} mobilization in cells expressing the receptor. Like other non-signaling chemokine receptors, CCRL2 displays structural changes in the DRYLAIV motif that is important for coupling receptors to G proteins (Bondue et al., 2011) (Mattern et al., 2014). CCRL2 is up-regulated by LPS and TNF-α, suggesting a role in the regulation of the immune system (Bondue et al., 2012). Zabel et al. proposed that

CCRL2 increases the local chemerin concentration and presents it to cells expressing ChemR23. CCRL2-transfected cells were indeed reported to enhance the mobilization of Ca^{2+} and receptor internalization following stimulation of cells expressing ChemR23 by chemerin (Zabel et al., 2008). Gonzalvo-Feo et al. showed a role of CCRL2 in the migration of DC through the endothelium. Endothelial cells produce chemerin and promote the adhesion of dendritic cells, by up-regulating CCRL2. In this study, CCRL2 was shown to concentrate bioactive chemerin at the surface of endothelial cells, promoting the migration of dendritic cells through the endothelium (Gonzalvo-Feo et al., 2014).

2. AIM OF THE PROJECT

Chemerin is a chemoattractant factor for immune cells, and is acting through three receptors, ChemR23, GPR1 and CCRL2. Its main function is to promote the migration of immune cells to inflamed tissues. Several studies have shown changes in circulating concentrations of chemerin in human cancers, suggesting a role of this chemoattractant molecule in the control of tumor progression. The aim of this project is to understand the role of chemerin and two of its receptors, CCRL2 and ChemR23, in tumor development. We will use mice deficient for each receptor, and the mice will receive grafts of tumor cell lines. We will observe the growth of tumors, as well as several processes affecting tumor growth, namely proliferation and apoptosis of tumor cells, the recruitment of immune cell populations, and the expression of angiogenic factors.

3. MATERIALS AND METHODS

3.1. ANIMALS

For all experiments, we used 6-10 week-old C57BL/6 mice, and groups included between 4 and 8 mice.

C57BL/6 is a mouse strain, which is widely used in scientific research. Its most significant advantage is to have its entire genome sequenced. Many disease models have also been established in this strain and genetically modified mouse lines are often available on this background. As main characteristics, the C57BL/6 mice present a low susceptibility to spontaneous tumors, making it therefore an excellent model for investigations in the cancer area, a high susceptibility to metabolic diseases, allowing the study of obesity and type 2 diabetes, a high incidence of hydrocephalus and microphthalmia, a low bone density and a good genetic stability (Mekada et al., 2009).

The ChemR23 knock-out mice (ChemR23$^{-/-}$) were obtained from DeltaGen (USA) and bred on the C57BL/6 background for more than ten generations, in order to obtain a pure genetic background. The CCRL2 knock-out mice (CCRL2$^{-/-}$) were provided by Silvano Sozzani, (University of Brescia, Italy) (Otero et al., 2010) and were bred on the C57BL/6 background for ten generations. All procedures involving animals were approved by the Ethical Committee of the Free University of Bruxelles, Belgium (CEBEA).

3.2. TUMOR CELL LINES

For assessing the role of receptors in tumor growth, two tumor cell lines were used: B16 melanoma cells and Lewis Lung Carcinoma cells (LLC).

The B16 cell line originates from a murine melanoma that developped in a C57/Bl6 mouse. It is therefore used as a syngeneic grafting model of melanoma in

C57/Bl6 mice. These cells can be grafted intradermally, subcutaneously or in foot pads. The B16 cells present a high capacity of local invasion and are highly metastatic, particularly although not exclusively to the lung (Bobek et al., 2010).

The LLC line was established from a spontaneous epidermoid carcinoma that developed in the lung of a C57/Bl6 mouse. The cell line is usually grafted in syngeneic animals (C57/Bl6 mice), in which it is highly tumorigenic and display a high capacity to metastasize, predominantly to the lung (Kellar et al., 2015).

Both cell lines were grafted into syngeneic C57BL/6 mice. The cell lines were grown in RMPI 1640 medium (Gibco, USA) containing 1% glutamine, 10% decomplemented fetal bovine serum (FBS, Gibco), 100 U/ml penicillin, 100 μg/ml streptomycin (Gibco), 1% non-essential amino-acids (Gibco) and 1% sodium pyruvate (Gibco), in an incubator at 37ºC and 5% CO_2.

3.3. GRAFTING OF TUMOR CELL LINES

Tumor cells were detached from the plates with a solution of 2% trypsin (Gibco) and 100 mM EDTA (Sigma, USA) in HBSS $CaCl_2$-$MgCl_2$ culture medium (Gibco, USA). Live cells were counted by the Trypan Blue dye exclusion test. 1.10^6 cells were injected subcutaneously in the back or flank of $ChemR23^{+/+}$, $ChemR23^{-/-}$, $CCRL2^{+/+}$ or $CCRL2^{-/-}$ mice. To follow tumor development, the size of tumors was measured daily following two perpendicular axes with a caliper, starting three days after injection, The tumor volume was estimated by the formula: .volume = 0.52 x $(width)^2$ x length.

3.4. TUMOR DIGESTION

Mice are sacrificed at different days, and the tumors were collected, cut into small pieces with scissors, and incubated in a digestion solution (10 mg/mL collagenase D (Roche, Switzerland), 2000 U/mL DNase I (Roche, Switzerland), 5% FBS in HBSS) for 1h30 at 37ºC, with gently agitation. The cell suspension was filtered through a 70 µm filter to remove residual debris, and centrifuged at 450 g for 5 minutes. The number of cells present in this suspension was counted in a Neubauer chamber, following staining of dead cells by the Trypan blue dye.

3.5. FLOW CYTOMETRY ANALYSIS

Flow cytometry is a powerful method that analyzes individual cell characteristics, by passing a large number of individual cells in rapid succession in front of a detector. Cells are labeled with specific antibodies coupled to fluorochromes with the aim of characterizing mostly cell surface markers, but also intracellular markers, present in the cell populations of interest (Jahan-Tigh et al., 2012).

This technique can be performed with blood leucocytes, cells differentiated in culture, or cell populations prepared from a variety of tissues, following digestion of the tissue and sieving through a mesh in order to obtain a cellular suspension. The cell suspension is incubated with antibodies coupled with fluorochromes such as fluorescein isothiocyanate (FITC), phycoerythrin (PE) or allophycocyanin (APC) (Jahan-Tigh et al., 2012).

The labeled cell suspension is thereafter introduced into the flow cytometer. The cells are passed through a narrow column that lines them one after the other. The fluorochromes are detected, following illumination by one or several laser beams, according to the wavelength of the emitted light, which is is analyzed by an optical system made of dichroic mirrors and detectors. Information on various surface

markers can therefore be collected simultaneously for the analysis of complex populations (Jahan-Tigh et al., 2012).

Besides the fluorescence data, the cytometer also records optical parameters: the forward scatter (FSC), which is a measure of the size of the cells, and the side scatter (SSC), indicating the granularity of the cells. This analysis is based on the angle of light emitted from the analyzed cells (Jahan-Tigh et al., 2012).

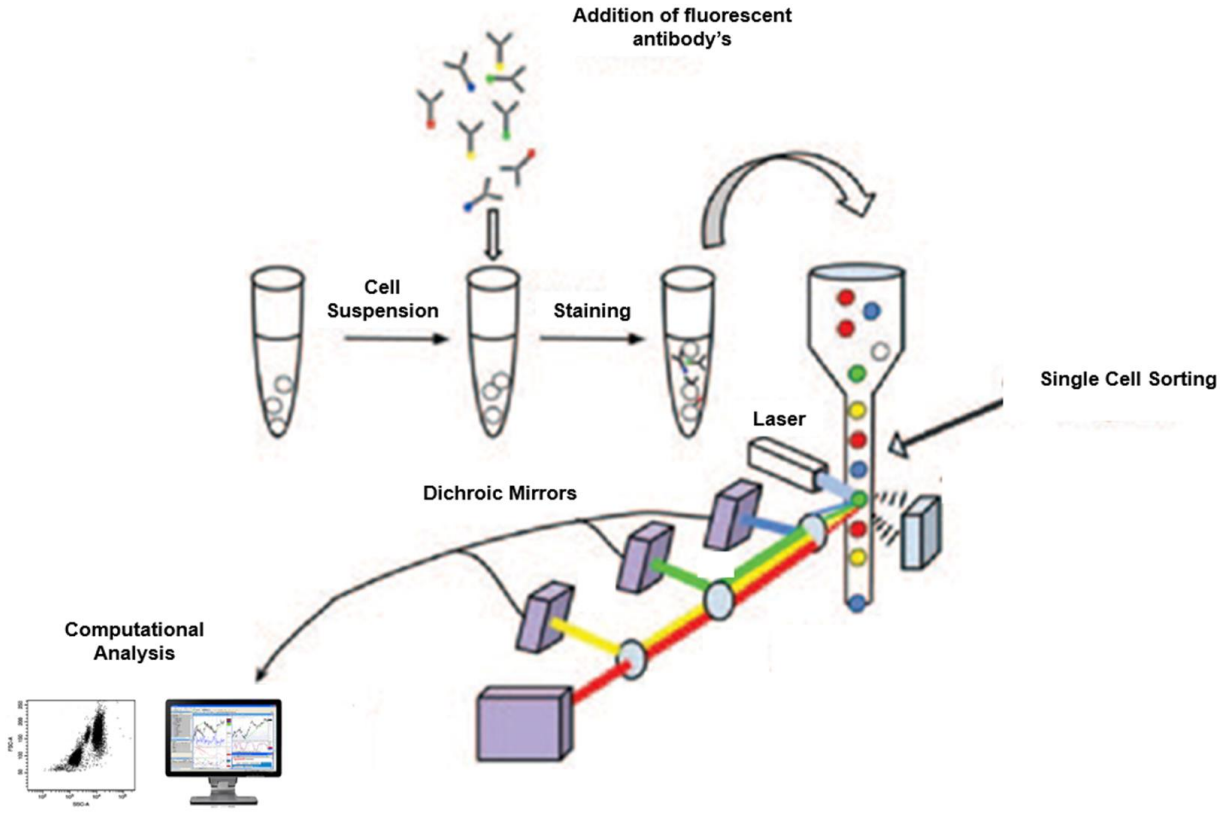

Figure 3.1 Flow cytometry. *The cell suspension is stained with fluorescent antibodies, and passed through the detection system. The light emitted by fluorochromes is passed through dichroic mirrors and various filters detected by a photomultiplier and transferred for analysis to a computer. The result of this analysis is displayed as histograms or two-dimensional dot-plots. [Adapted from Brown et al. (2000) and Jahan-Tigh et al. (2012)]*

In this work, to determine the different subsets of leukocytes present in tumors, the cells isolated from tumors were stained with fluorescent dye-labeled antibodies and analyzed by flow cytometry. 2.10^5 cells were resuspended in 100 µL of FACS solution (1% FBS, 5 mM EDTA in PBS) and centrifuged at 450 g for 5 minutes at 4ºC. To block unspecific binding, the cells were incubated with anti-CD16/CD32 antibodies for 20 minutes at 4ºC, are washed by centrifugation at 450 g for 5 minutes at 4ºC. For staining of cell membrane markers, the following antibodies were used: FITC- (Fluorescein Isothiocyanate), R-PE- (R-Phycoerythrin), APC- (Allophycocyanin) or APC/Cy7- (Allophycocyanin/cyanine 7) conjugated anti-CD45; APC-conjugated anti-CD3; R-PE/Cy7- (R-phycoerythrin/cyanine 7) conjugated anti-TCR; A488- or V450-conjugated anti-CD4; PerCP/Cy5.5- (Peridinin Clhorophyll Protein Complex/Cyanine 5.5) or V500-conjugated anti-CD8; FITC- or PerCP/Cy5.5-conjugated anti-CD11b; PerCP/Cy5.5- or R-PE/Cy7-conjugated anti-Gr1; PE-conjugated anti-Ly6G; EF450-conjugated anti-Siglec H; R-PE/Cy7-conjugated anti-B220; V450- or APC-conjugated anti-CD11c; FITC- or EF450-conjugated anti-F4/80; PE-conjugated anti-CD49b antibodies (eBioscience, USA). Viability dye 7-AAD (eBioscience, USA) and Hoescht 33342 (Life Technologies, USA) were used to stain live cells.

For staining of intracellular markers, the cells were fixed with 2% paraformaldehyde (PFA) for 15 minutes, and permeabilized in 0.5% saponine in FACS solution. Cells were further incubated with FITC-conjugated Ki67 antibody (eBioscience, USA) for 45 minutes. After a washing step, the cells were analyzed on a FacsAria II flow cytometer (Becton Dickinson, USA).

To identify apoptotic cells, 2.10^5 cells were incubated with eF450-conjugated anti-annexin V antibody for 15 minutes at room temperature (RT) in the dark. Cells were washed twice and resuspended in FACs buffer. The viability dye 7-AAD was added and cells were analyzed on a FacsAria II flow cytometer.

3.6. IMMUNOFLUORESCENCE MICROSCOPY

Immunofluorescence microscopy is a highly used technique in scientific research, through the use of fluorescent antibodies that allow detecting specific target antigens. There are two types of immunofluorescence labeling, direct and indirect. Direct immunofluorescence (DIF) refers to the use onto the tissue of fluorescently tagged antibodies directed against the target antigen. Indirect immunofluorescence requires two successive steps. First, a primary antibody, which is not tagged, binds to the target antigen. Then, a secondary antibody labeled fluorescently, binds to the primary antibody, and thus, and generates a specific staining. This technique is a bit more complex than the first, because it involves more incubation steps, but it is more sensitive, because of the amplification step brought by the secondary antibody. It is therefore less affected by the nonspecific auto-fluorescence that is observed in some tissues (Odell et al., 2013).

In this project, we have used confocal microscopy instead of conventional microscopy, because confocal microscopy has several advantages that conventional fluorescence microscopy has not. The conventional microscope has as major disadvantage that only thin sections can be visualized, requiring the use of fixative agents and embedding media or freezing the samples prior to sectionning. Confocal microscopy creates virtual sections through much thicker samples, providing high quality images and an increased level of details than conventional microscopy, starting from unfixed and possibly live tissues. In confocal microscopy, an intense input light beam illuminates the samples in a scanning mode, but only the emitted light originating from a specific plane in the sample is focused through the lens of the microscope ans visualized. The light emitted outside the focal plane is blocked by passage through a narrow pinhole, in order to make easier the visualization of the focal plane. Focused planes are scanned and reconstructed by a computer system, and several planes can be combined to reconstruct three-dimensional images (Nwaneshiudu et al., 2012).

In this work, tumors were embebbed in OCT (Sakura, Japan) and stored at -80ºC. Tumor cryosections of 8-12 µm were made and placed on Superfrost Plus slides (Thermo Scientific, USA). Sections were fixed in acetone for 10 minutes and air dried for 2-3 hours. To block unspecific binding, sections were incubated in a solution of 3% BSA and 0.1% Triton X100 in PBS. We used APC-conjugated anti-CD45, FITC-conjugated anti-Ki67, PE-conjugated anti-CD31, purified anti-cleaved caspase 3 (eBioscience) and A488-conjugated rabbit anti-IgG (Life Technologies, USA) antibodies. The slides were mounted with coverslips and mounting medium (2% Glycergel Dabco , Sigma, USA). Tumor sections were analyzed on a Zeiss LSM 780 confocal microscope (Zeiss, Germany), and the images collected and analyzed by Carl Zeiss Microscopy and Image J softwares.

3.7. HEMATOXYLIN/EOSIN STAINING

Hematoxylin and eosin coloration constitutes the most classical staining procedure for histological examination of tissue samples. It allows the recognition of different cell types and their organization in tissues, as well morphological changes, thus allowing the diagnosis of various diseases such as cancer. This technique is therefore useful for complementing the analysis of tissues by immunofluorescence in order to visualize the overall structure of the analyzed samples, which is not always obvious from immunofluorescence data (Fisher et al., 2006).

This procedure allows to stain intracellular complements such as the nucleus and the cytoplasm and delimits the cells by highlighting the cellular membranes. Hematoxylin stains nucleic acids, because of its affinity for basophilic substances, resulting in a blue/purple staining. Eosin has affinity to acidophilic substances and labels non-specifically proteins by a pink staining. Thus, in a normal tissues, the nuclei are stained blue, while the cellular membrane and cytoplasm display different shades of pink (Fisher et al., 2006).

In this work, the tumor sections were passed successively into 90% isopropanol, an hematoxylin solution, 0.5% lithium carbonate, 1% eosin Y solution, 70%, 90% and 100% ethanol, toluene (VWR Chemicals, USA) before mounting with coverslips and Entellan solution (Merck, USA). Sections were analyzed on a AxioImager Z1 microscope (Zeiss, Germany) and the images obtained were treated by AxioVision and Image J softwares.

3.8. ELISA

Enzyme-linked immunosorbent assays (ELISA) are important tools for biomedical research, but also for medical diagnosis. These assays have the ability to detect all types of biological molecules at minimal concentrations (Gan et al., 2013).

An antigen binding antibody is coated on a solid surface allowing the binding of target molecules. The antigen, which is added in the liquid phase, is detected by a specific antibody, which in turn is detected by a secondary antibody. The secondary antibody is linked to the generation of a chromogenic substrate, which allows a color or fluorescence change, indicating the presence of antigen. The level of fluorescence is measured by a spectrophotometer, quantitatively or qualitatively. There are four types of ELISA: indirect, competitive, sandwich and multiple, but we focus in the sandwich technique (Gan et al., 2013).

Sandwich ELISA is used to recognize a specific antigen in a sample. A microtiter plate is coated with a capture antibody specific to the target antigen. Non-specific binding is blocked with bovine serum. The sample is added, followed by the primary antibody specific for the target antigen. The secondary antibody, coupled to an enzyme, then binds to the primary antibody. Subsequently, the substrate is added to allow reaction with the enzyme, and cause a change in color or fluorescence. This technique has the advantage of using two antibodies specific for the antigen of interest, thereby increasing its specificity (Gan et al., 2013).

In our experiments, the concentration of total chemerin in mouse plasma was assessed by a Sandwich ELISA (R&D Systems, USA). Blood from CCRL2 $^{+/+}$ and $^{-/-}$ mice was collected in presence of 0.5M EDTA and centrifuged for 10 minutes at 300 g, and the plasma was recovered. Wells from 96 well plates were coated overnight at RT with 4 µg/mL purified anti-chemerin antibody diluted in PBS. The plates were washed with a wash buffer (0.05% Tween 20 in PBS) and unspecific binding sites blocked with 1% BSA in PBS for 1 hour at RT. After washing, recombinant chemerin (used as standard) and experimental samples were diluted in PBS containing 1% BSA and incubated in the wells for 2 hours at RT. Biotinylated anti-chemerin antibody (1 µg/mL) was added and incubated for 2 hours at RT. The plate was washed and streptavidin-HRP (Horseradish peroxidase, R&D Systems, USA) was added for 20 minutes at RT in the dark. After washing, the substrate solution (H_2O_2 + 3,3′,5,5′-tetramethylbenzidine, TMB) was added for 20 minutes at RT in the dark. The reaction was stopped by addition of 2 N H_2SO_4. The optical density was measured on a Biorad spectrophotometer at 450 nm (reference 570 nm).

3.9. RT-QPCR

Retro-transcriptase quantitative PCR allows the analysis of gene expression by the assaying the amount of a specific RNA species in cells or tissues. The RNA is first retro-transcribed into complementary DNA (cDNA), which, in turn, is amplified by PCR, and the amount of the PCR product is quantified along the cycles.

In this work, the main objective is the amplification of a number of specific genes used as markers of inflammation or angiogenesis. Thus, we used specific primers (forward and reverse) for each of these genes. To visualize the amplification in real-time, either fluorescent dsDNA binding dyes (such as SYBR Green) or fluorescent probes (TaqMan) are used. Thus, the amplified genetic sequences emit fluorescence, which is recorded during the amplification process, and these data

are transferred to a computer analysis system. This powerful technique allows then the quantitative analysis of mRNA for a given gene (Gentle et al, 2001).

This quantification may be absolute or relative. The absolute quantification allows knowing the number of copies of a specific transcript through the use of a reference curve, which is normally done with different amounts of a plasmid containing the sequence of interest. The relative quantification of expression correlates the amount of target sequence with the expression of one or several reference genes that are not expected to vary too much from tissue to tissue or in different experimental conditions. These reference genes are usually chosen amongst housekeeping gene, provided the relative stability of their expression. This second method is used to compare changes in the expression of a gene in different samples (Santos et al., 2004).

To extract RNA from the tumors, the tumors were sonicated in 1 mL of Trizol solution (Invitrogen, UK) in RNase-free tubes, and stored at -80ºC. After thawing, 200 µL of chloroform was added to the samples, and the tubes were centrifuged at 12000 rpm for 15 minutes at 4ºC. The upper phase was transferred to a new tube, and 500 µL of isopropanol was added to precipitate RNA. The samples were incubated 10 minutes at RT, and centrifuged at 12.000 rpm for 10 minutes at 4ºC. The supernatant was removed and 1 mL of 75% ethanol was added. The samples were centrifuged at 7500 rpm during 5 minutes at 4ºC. The supernatant was completely removed, and the pellets were air dried for 30 minutes. The pellet was next resuspended in 20 µL of RNAse free water. The concentration of RNA is measured in a Nanodrop (USA). Complementary DNA (cDNA) was obtained from 2 µg of mRNA by reverse transcription using SuperScript III (Invitrogen, UK) according manufacturer's instructions.

The expression of angiogenic and inflammatory factors was determined by relative quantitative PCR (qPCR) using SYBR Green Power kit (Invitrogen, UK) and using the primers listed in Table 3.1. The qPCR thermocycling conditions for all genes were 10 min at 95˚C, followed by 40 cycles of denaturation at 95˚C,

annealing at 60˚C and extension at 72˚C, all for 15 sec. The quantitative PCR was performed using a 7500 Real-Fast thermocycler (Applied Biosystems, USA). The expression levels were normalized using GAPDH as a reference housekeeping gene.

Table 3.1. Primers of angiogenic and inflammatory factors used in quantitative RT-PCR experiments.

Gene		**Terminal**	**Sequence**
Glyceraldehyde-3-Phosphate Dehydrogenase	mGAPDH	fw	AAG-GGC-TCA-TGA-CCA-CAG-TC
	mGAPDH	rev	CAG-GGA-TGA-TGT-TCT-GGG-CA
Thrombospondin 1	mTSP1	fw	ACT-TCA-CCT-TTG-CCA-CCT-C
	mTPS1	rev	AGA-CTC-TGG-AAT-GCG-GTT-G
Vascular Endothelial Growth Factor A	mVEGFA	fw	GGC-AGC-TTG-AGT-TAA-ACG-AAC
	mVEGFA	rev	TGG-TGA-CAT-GGT-TAA-TCG-GTC
Fibroblast Growth Factor 2	mFGF2	fw	TCT-ACT-GCA-AGA-ACG-GCG
	mFGF2	rev	CTC-CCT-TGA-TAG-ACA-CAA-CTC-C
Transforming Growth Factor, Beta 1	mTGFb	fw	GGA-GAG-CCC-TGG-ATA-CCA-AC
	mTGFb	rev	CAA-CCC-AGG-TCC-TTC-CTA-AA
Interleukin 10	mIL10	fw	ATT-TGA-ATT-CCC-TGG-GTG-AGA-AG
	mIL10	rev	CAC-AGG-GGA-GAA-ATC-GAT-GAC-A
Interleukin 6	mIL6	fw	TCC-AGT-TGC-CTT-CTT-GGG-AC
	mIL6	rev	GTA-CTC-CAG-AAG-ACC-AGA-GG
Interleukin 1b	mIL1b	fw	CAC-AGC-AGC-ACA-TCA-ACA-AG

	mIL1b	rev	GTG-CTC-ATG-TCC-TCA-TCC-TG
Tumor necrosis factor alpha	mTNFa	fw	ATG-AGA-AGT-TCC-CAA-ATG-GC
	mTNFa	rev	CTC-CAC-TTG-GTG-GTT-TGC-TA
Matrix Metalloprotease 9	mMMP9	fw	TAA-GGA-CGG-CAA-ATT-TGG-TT
	mMMP9	rev	CTT-TAG-TGG-TGC-AGG-CAG-AG
Matrix Metalloprotease 10	mMMP10	fw	CCT-GTG-TTG-TCT-GTC-TCT-CCA-AGA
	mMMP10	rev	CGT-GCT-GAC-TGA-ATC-AAA-GGA-C
Chemokine (C-X-C Motif) Ligand 1	mCXCL1	fw	TGC-ACC-CAA-ACC-GAA-GTCA-T
	mCXCL1	rev	TTG-TCA-GAA-GCC-AGC-GTT-CAC
Chemokine (C-X-C Motif) Ligand 2	mCXCL2	fw	CGC-TGT-CAA-TGC-CTG-AAG
	mCXCL2	rev	GGC-GTC-ACA-CTC-AAG-CTC-T
Chemokine (C-C Motif) Ligand 2	mCCL2	fw	AAC-TCT-CAC-TGA-AGC-CAG-CTC-T
	mCCL2	rev	CGT-TAA-CTG-CAT-CTG-GCT-GA
Hypoxia Inducible Factor 1, Alpha Subunit	mHIF1a	fw	GGT-TCC-AGC-AGA-CCC-AGT-TA
	mHIF1a	rev	AGG-CTC-CTT-GGA-TGA-GCT-TT

3.10. HIGH PRESSURE LIQUID CHROMATOGRAPHY (HPLC)

Chromatography is an analytical technique that allows separation of different molecules on the basis of their structure and/or physicochemical properties. The sample passes through a stationary phase where the molecules will have different interactions with the support, leading to the separation of molecules (Kupiec, 2004).

The HPLC instrumentation consists of pumps, injectors for the samples, columns, detectors and a display system. The main component is the column where the chromatographic separation occurs. The pump, allowing to apply high pressure onto the column, is necessary to transport efficiently the mobile liquid phase containing the components through the fixed phase of the column. The samples are introduced into the liquid phase through an injector loop. The detection method used to analyze the components separated by the column is very important and needs to be adapted to the nature of the molecules of interest. Fractions of the liquid phase flowing out of the column are collected for further analysis or subsequent purification steps (Kupiec, 2004).

In our experiments, the aim was to purify chemerin from mouse plasma samples. For this purpose, we used an HPLC setting with a heparin column. Heparin is a negatively charged polysaccharide, thereby allowing binding of positively charged biomolecules such as enzymes, growth factors, hormones or chemokines. Chemerin is known to bind heparin efficiently and this column is therefore well adapted for a first purification step. Heparin columns constitute an absorption chromatography, which is useful to concentrate molecules at low concentrations in the starting sample, as is the case of active chemerin in the blood (Xiong et al., 2008).

In order to detect the bioactive chemerin in the HPLC fractions, we used a calcium-mobilization assay based on the bioluminescence of aequorin. The aequorin-based assay enables the analysis of the interaction of proteins with GPCRs coupled to the release of intracellular Ca^{2+}. In this assay, we used cells expressing apoaequorine, the Gα16 protein subunit, allowing to redirect the coupling of most GPCRs toward phospholipase C, and the target receptor (in this case, ChemR23). The cells are incubated with coelenterazine (the apoaequorine cofactor) in order to reconstitute the active enzyme aequorin. The aequorin is activated by the increase in cytosolic Ca^{2+}, following activation of the receptor by its ligand. This creates a rapid and transient luminescence signal, which is

proportional to the calcium concentration and is recorded by a luminometer. Thus, activation of the recombinant GPCR expressed in the reporter cell line results in the generation of aequorin bioluminescence, which is recorded by a luminescence reader (Oksa et al., 2009).

The concentration of bioactive chemerin in the blood of CCRL2$^{+/+}$ and $^{-/-}$ mice was following fractionation of the samples by HPLC. The plasma samples were diluted ten times in a 20 mM phosphate buffer (pH 8.0) and filtered through 4 µm, 0.45 µm and 0.22 µm filters. The samples were placed on a HiTrap Heparin HP column (GE Healthcare) with a capacity of 1 mL. The elution was performed with a gradient of NaCl (20 to 700 mM), and 1 mL of fractions were collected. CHO (Chinese hamster ovary) cells, expressing ChemR23, apoequorin and $G_{\alpha 16}$, were collected from culture dishes, resuspended in an aequorin buffer (DMEM containing 0.5% BSA and 5 µM coelenterazine H) and incubated for 4 hours under gentle agitation in the dark. The cells (50,000 cells in 50 µL) were added to wells containing different concentrations of the collected fractions or recombinant mouse chemerin used as standard. The luminescence was measured for 30 s in a LB 960 luminometer (Berthold Technology). The results were normalized to the response obtained with 20 µM ATP acting through endogenous receptors of CHO cells.

3.11. STATISTICAL ANALYSES

Statistical significance was calculated by using the Mann-Whitney U test or Wilcoxon test, with the GraphPad Prism 6 software.

The Mann-Whitney test is a non-parametric test used to compare the distribution of a variable using two independent samples. It is used as an alternative to the Student t test for independent testing, when the number of samples is low or too different across groups, or when the variances are heterogeneous (Rank et al., 1988).

The Wilcoxon test is a non-parametric test used when two independent groups are submitted to the same conditions. This test is appropriate when analyzing the data of repeated measurements made in two conditions (Grok, n.d.).

For both tests, the differences were considered significant at P value < 0,05 (* represent p value < 0,05).

4. RESULTS

The aim of this project is to understand the influence of chemerin receptors, ChemR23 and CCRL2, in a mouse model of tumorigenesis. We use mice deficient for each of these receptors and grafted them with tumor cell lines to observe the influence of the receptors on tumor implantation, immune cell recruitment and angiogenesis. Two tumoral cell lines derived from C57Bl6 mice were used, the B16 melanoma and Lewis lung carcinoma (LLC) cell lines.

4.1 CHEMR23 IS NOT INVOLVED IN THE CONTROL OF B16 TUMOR DEVELOPMENT

ChemR23 is the main receptor of chemerin. It is described to induce the migration of immune cell populations known to influence tumor progression, such as NK cells, macrophages and dendritic cells (Vermi et al., 2005). To analyze the effect of ChemR23 deficiency on tumor development, 1.10^6 B16 tumor cells were injected in the flank of $ChemR23^{+/+}$ and $ChemR23^{-/-}$ mice, and we measured the tumor growth during ten days after tumor implantation (Figure 4.1).

We observed that tumors from $ChemR23^{+/+}$ and $ChemR23^{-/-}$ mice became detectable and developed with the same time frame. These data suggest that ChemR23 does not play a major role in the control of tumor development, at least in this particular model. ChemR23 allowing the migration of dendritic cells, NK cells and macrophages, we determined whether the absence of ChemR23 affects the immune cell recruitment to the tumor site.

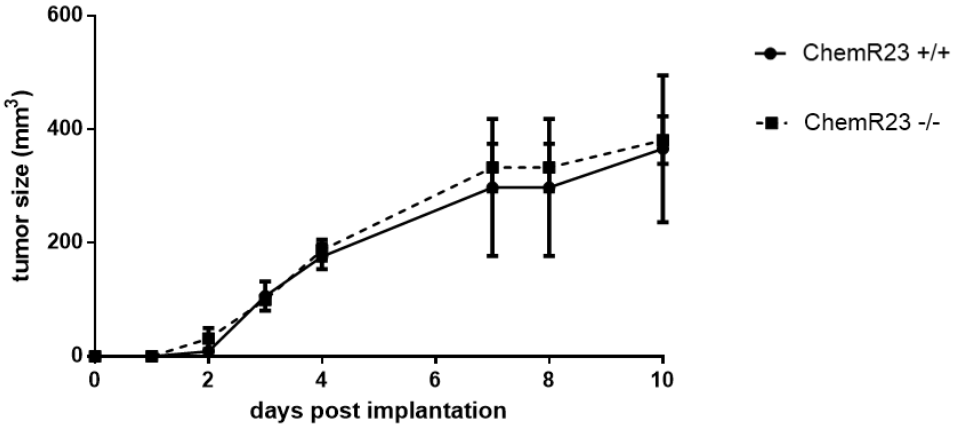

Figure 4.1 ChemR23$^{+/+}$ (n=5) and ChemR23$^{-/-}$ (n=5) mice develop tumor in a similar way. *1.10^6 B16 cells were injected subcutaneous into ChemR23$^{+/+}$ (circle) and $^{-/-}$ (square) mice. The size of tumors was measured daily for 10 days after cell implantation. The tumor size is calculated according to the formula: Volume = 0.52 x (width)^2 x length. This experiment is representative of 3 independent experiments.*

Ten days after tumor implantation, tumors were removed and digested, and immune cell populations infiltrating the tumors were identified by flow cytometry. We first analyzed the recruitment of CD45-positive cells as a measure of total immune cells (Figure 4.2 A). No difference was observed between ChemR23$^{+/+}$ and ChemR23$^{-/-}$ mice. We next analyzed the different subsets of immune cells among the CD45$^+$ population. The proportion of macrophages (CD11b$^+$ F4/80$^+$ CD11c$^-$ cells), myeloid dendritic cells (CD11c$^+$ Siglec H$^-$ cells), plasmacytoid dendritic cells (CD11c$^+$ Siglec H$^+$ cells), MDSC (CD11b$^+$ Gr1$^+$ cells), T cells (CD3$^+$ cells) and NK cells (NK1.1$^+$ CD3$^-$ cells) were not significantly different between the two groups (Figure 4.2 B-E). These results show that ChemR23 does not affect significantly the recruitment of immune cells in this model. They are consistent with the absence of effects on tumor growth, and suggest that ChemR23 does not play a major role in tumor development neither in the immune cell recruitment to the tumor site in this B16 melanoma model.

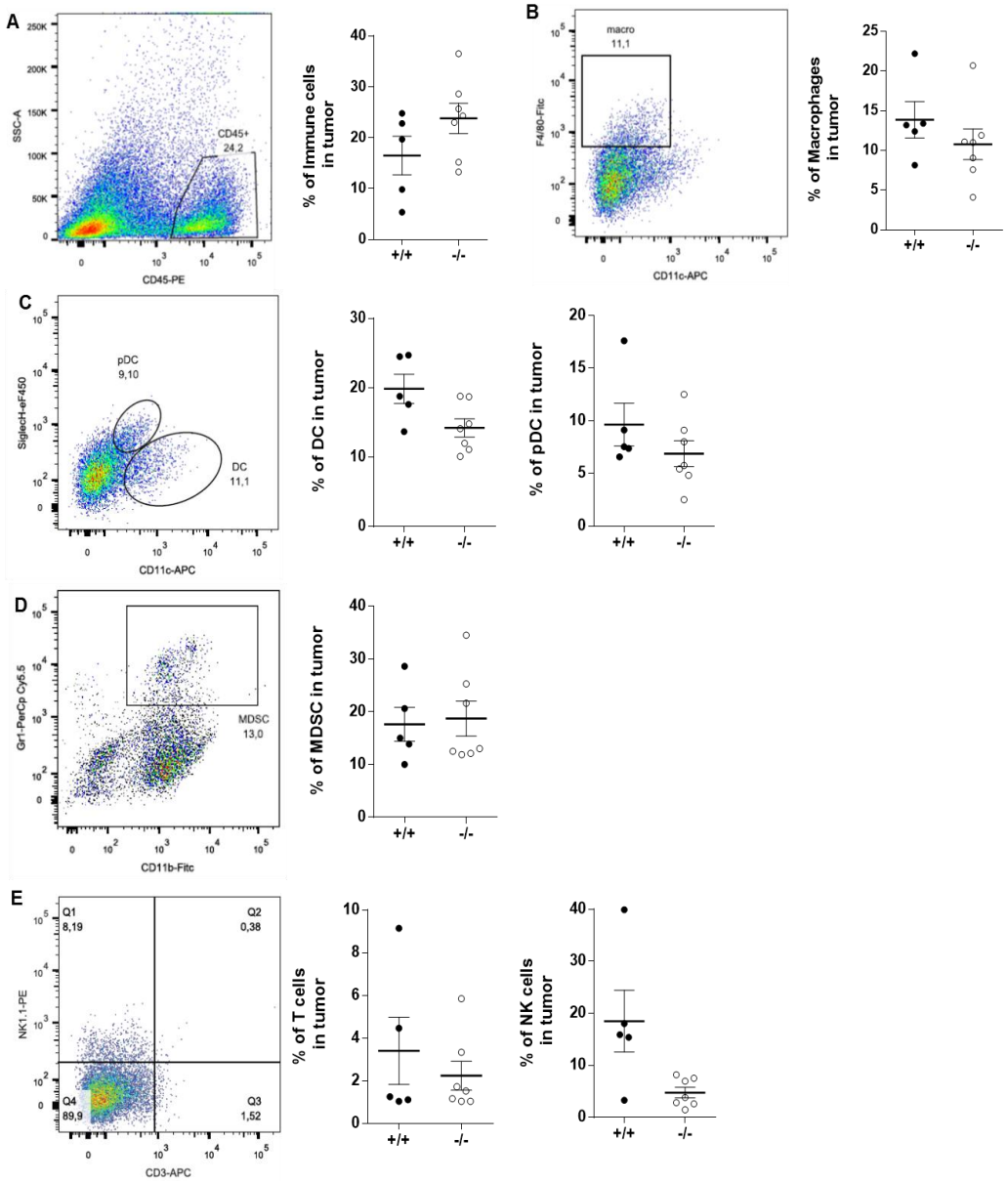

Figure 4.2. The immune cell recruitment to B16 tumors is not affected by ChemR23*. 1.10^6 B16 cells were injected subcutaneously in the back of ChemR23$^{+/+}$ and $^{-/-}$ mice. The mice were sacrificed 10 days later, and the tumors were removed and digested. The immune cell populations were analyzed by flow cytometry. (**A**) Percentage of total immune cells (CD45$^+$). (**B-E**) Proportion of immune cells subsets among the CD45$^+$ population: macrophages (CD11b$^+$ F4/80$^+$ CD11c$^-$), myeloid dendritic cells (CD11c$^+$ Siglec H$^-$), plasmacytoid dendritic cells (CD11c$^+$ Siglec H$^+$), MDSC (CD11b$^+$ Gr1$^+$), T cells (CD3$^+$) and NK cells (NK1.1$^+$ CD3$^-$). This experiment is representative of 3 independent experiments. None of the differences between the two groups was statistically significant.*

4.2 THE ABSENCE OF CCRL2 LEADS TO A DECREASE IN TUMOR GROWTH.

Previous results suggested that the protective effects of chemerin on tumor development demonstrated both in the host laboratory and in the literature (Pachynski et al, 2012) are not entirely mediated by ChemR23. Chemerin is also able to bind CCRL2 , which is also expressed on immune cells. In order to determine whether CCRL2 is involved in the control of tumor development, 1.10^6 B16 cells were injected in $CCRL2^{+/+}$ and $CCRL2^{-/-}$ mice, and we measured the tumor growth during ten days after tumor implantation (Figure 4.3 A). $CCRL2^{+/+}$ and $CCRL2^{-/-}$ mice developed tumors at about the same time, but the tumors remained smaller in $CCRL2^{-/-}$ mice than in $CCRL2^{+/+}$ mice. These data suggest that CCRL2 has a pro-tumoral effect in this particular model. To confirm the effects of CCRL2 on tumor development, we used another tumor cell line, the Lewis lung carcinoma cell line (LLC). 1.10^6 cells were injected subcutaneously in $CCRL2^{+/+}$ and $^{-/-}$ mice and the tumor size was measured daily (Figure 4.3 B). We observed the same effect of CCRL2-deficiency as for B16 tumors, with a slower growth rate in $CCRL2^{-/-}$ mice.

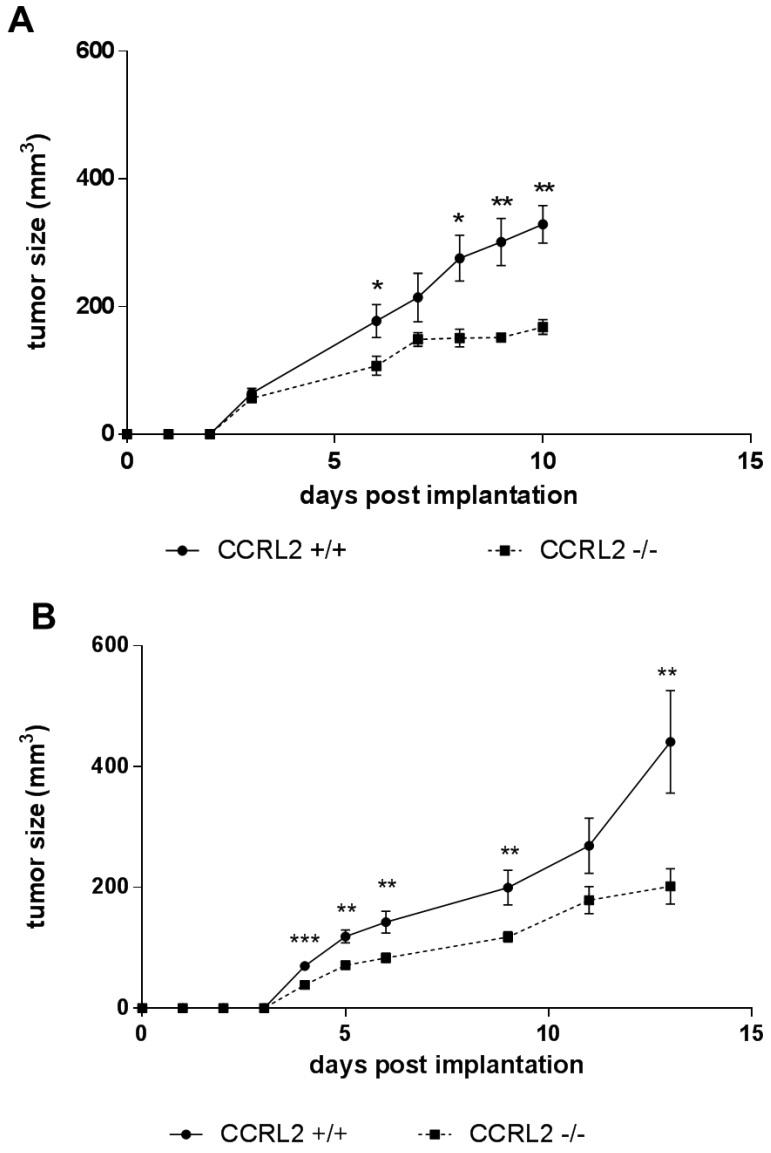

Figure 4.3. B16 and LLC tumors develop more slowly in CCRL2-deficient mice (A) *CCRL2$^{+/+}$ and CCRL2$^{-/-}$ mice were injected with B16 cells and sacrificed ten days after implantation (n=8 per group)* ***(B)*** *CCRL2$^{+/+}$ and CCRL2$^{-/-}$ mice were injected with LLC cells and sacrificed 13 days after implantation (n=5 per group). The statistical test used is a Mann-Whitney test. *,** and *** represent respectively p values of < 0.05, < 0.01 and < 0.001.*

4.3 THE PLASMA CHEMERIN CONCENTRATION IS NOT ALTERED IN CCRL2-DEFICIENT MICE

CCRL2 is expressed in immune cells, however this receptor is described as non-functional (Bondue et al., 2012). A potential role of CCRL2 could be the presentation of chemerin to Chem23-expressing cells (Yoshimura et al., 2010). Binding of chemerin to CCRL2 could therefore affect the distribution of chemerin and affect the concentration of the protein in the circulation. To better understand how CCRL2 affects tumor development, we therefore determined the consequences of CCRL2 deficiency on the plasma concentration of chemerin. Blood samples were collected from $CCRL2^{+/+}$ and $CCRL2^{-/-}$ mice and total chemerin levels were measured by ELISA. We observed the same concentration of plasmatic total chemerin in $CCRL2^{+/+}$ and $CCRL2^{-/-}$ mice. These results suggest that plasmatic chemerin is not affected by the presence or absence of CCRL2 (Figure 4.4 A).

Prochemerin is the major form of circulating chemerin in the blood. Chemerin becomes active after cleavage by proteases, in particular in an inflammatory context. We assessed the concentration of bioactive chemerin from plasma in $CCRL2^{+/+}$ and $CCRL2^{-/-}$ mice. Chemerin was purified by chromatography on a heparin column, and its activity was evaluated by a calcium-mobilization assay based on the luminescence of aequorin. In Figure 4.4B, we observed that the concentration of bioactive isoforms of chemerin in CCRL2 $^{/+}$ and $CCRL2^{-/-}$ mice is similar. These results show that plasmatic levels of bioactive chemerin are not affected by the absence of this receptor. With these results, we can conclude that the concentrations of bioactive chemerin or its inactive precursor are not changed between $CCRL2^{+/+}$ and $CCRL2^{-/-}$ mice in basal conditions.

We next determined whether the tumor development affects the levels of chemerin. Three days after tumor cell implantation, blood samples were collected from $CCRL2^{+/+}$ and $CCRL2^{-/-}$ mice, and chemerin levels were quantified by ELISA.

We found that chemerin levels were moderately increased in tumor-bearing animals (Figure 4.4 C), when compared to basal conditions (Figure 4.4 A). The increase was however similar in the two groups, suggesting that chemerin levels are not affected by CCRL2 in a tumoral context.

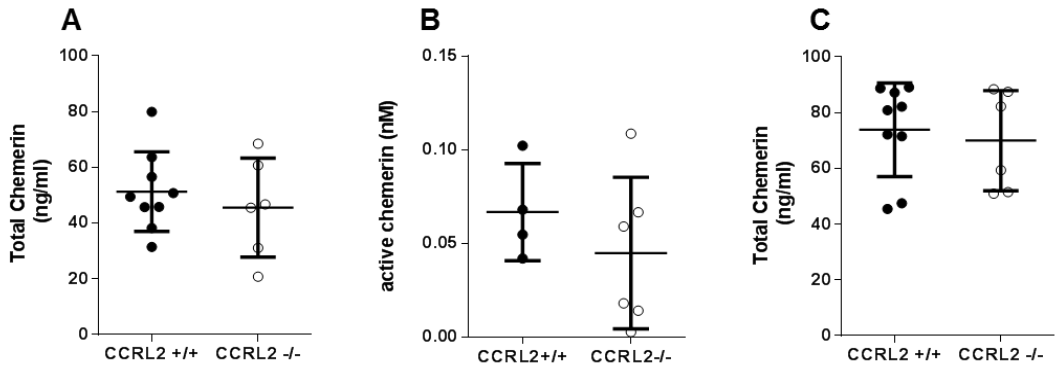

Figure 4.4. The circulating levels of chemerin are not altered in CCRL2 knock-out mice. *Blood samples were collected from CCRL2$^{+/+}$ and CCRL2$^{-/-}$ mice, and plasma was recovered. The levels of total and bioactive chemerin were measured by ELISA and a functional assay based on aequorin luminescence, respectively.* ***(A)*** *Total chemerin concentration in CCRL2$^{+/+}$ and CCRL2$^{-/-}$ mice, in basal conditions, by ELISA.* ***(B)*** *Active chemerin concentrations in CCRL2$^{+/+}$ and CCRL2$^{-/-}$ mice, in basal conditions, by the aequorine-based assay.* ***(C)*** *Total chemerin concentration in CCRL2$^{+/+}$ and CCRL2$^{-/-}$ mice, three days after B16 tumor implantation.*

4.4 CCRL2 DOES NOT AFFECT THE IMMUNE CELL RECRUITMENT TO B16 AND LLC TUMORS

CCRL2 is expressed on immune cells such as plasmacytoid dendritic cells, mast cells and macrophages. To understand the effect of CCRL2 in anti-tumor immunity, we analyzed the recruitment of immune cells to B16 tumors. The tumors developed by CCRL2$^{+/+}$ and CCRL2$^{-/-}$ mice are removed and digested ten days after implantation, and the main immune cell subsets were analyzed by flow cytometry.

We first analyzed the recruitment of total immune cells (CD45-positive cells), and no difference was observed between the two groups of mice (Figure 4.5). We

next analyzed the different subsets of immune cells among $CD45^+$ cells. The proportion of macrophages, myeloid dendritic cells, plasmacytoid dendritic cells, MDSC, T cells and NK cells were similar in $CCRL2^{+/+}$ and $CCRL2^{-/-}$ mice (Figure 4.5), suggesting that CCRL2 does not affect significantly the recruitment of immune cells in this model.

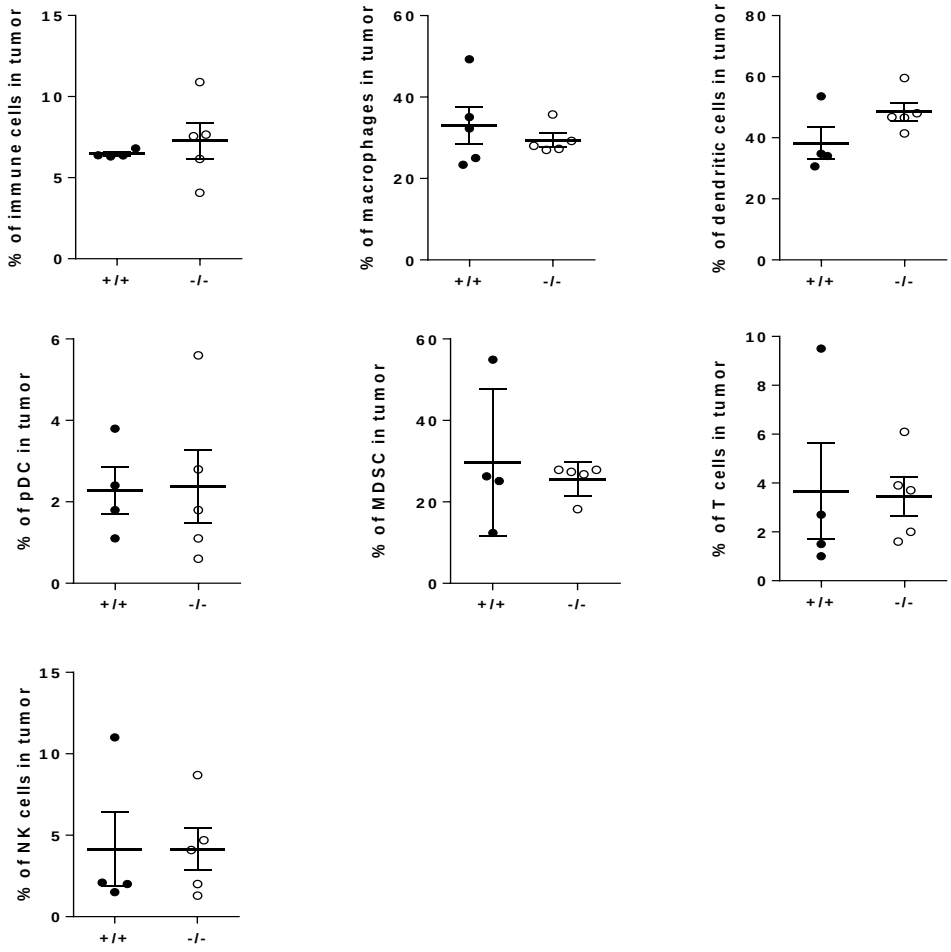

Figure 4.5 The immune cell recruitment to B16 tumors is not affected by CCRL2, at day 10 of tumor growth*. 1.10^6 B16 cells were injected subcutaneously in the back of $CCRL2^{+/+}$ and $CCRL2^{-/-}$ mice. The mice are sacrificed 10 days after, the tumors were collected and digested. The first graph shows the percentage of total immune cells ($CD45^+$), and the next graphs are representative of immune cells subsets: macrophages ($CD11b^+$ $F4/80^+$ $CD11c^-$), dendritic cells ($CD11c^+$ $CD11b^+$), plasmacytoid dendritic cells ($CD11c^+$ Siglec H^+), MDSC ($CD11b^+$ $Gr1^+$), T cells ($CD3^+$) and NK cells ($NK1.1^+$ $CD3^-$). This data set is representative of 3 independent experiments.*

We postulated that CCRL2 could affect the immune cell recruitment only at early stages of tumor development. We therefore performed the same experiment, but collected the tumors at day 3 and day 6 of tumor development. We observed that the total number of immune cells (Figure. 4.6 A) present in the tumor is similar between $CCRL2^{+/+}$ and $CCRL2^{-/-}$ mice, at day 3 and day 6 of tumor development. We also characterized several subsets of immune cells. The proportion of NK cells, dendritic cells ($CD11c^{+}$ $CD11b^{+}$), and total $CD11b^{+}$ cells (including macrophages and MDSC) were similar in $CCRL2^{+/+}$ and $CCRL2^{-/-}$ mice, in the two time points (Figure 4.6 B-E).

These results suggest that CCRL2 does not affect the proportion of immune cell recruitment at different stages of tumor development. We confirmed our results by performing immunofluorescence staining of immune cells on tissue sections, to determine the distribution of the populations in the tumor and its microenvironment. The tumors were recovered from wild-type and CCRL2 knock-out mice at day 3 and day 6 of tumor development. Sections of tumors were staining with an anti-CD45 antibody to identify immune cell. The proliferating tumor cells were identified with an anti-Ki67 antibody.

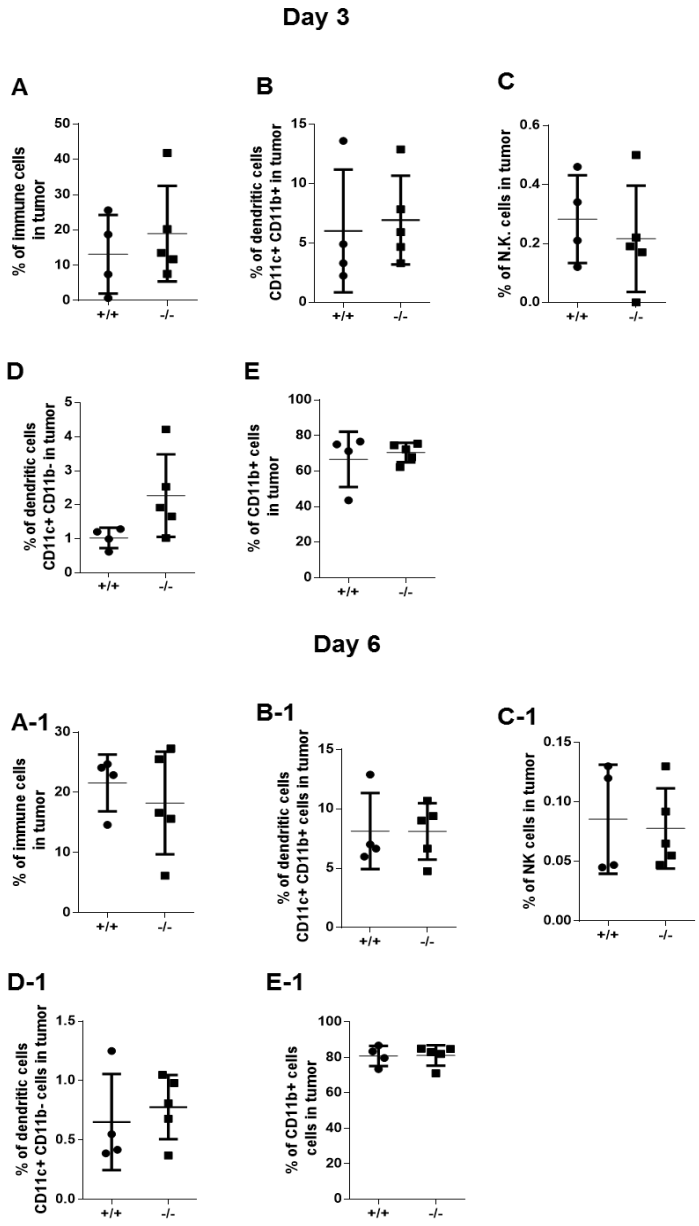

Figure 4.6. The immune cell recruitment to tumors is not affected by CCRL2, at day 3 (top panels) and day 6 (bottom panels) of tumor growth. *1.10^6 B16 cells were injected subcutaneously in the back of $CCRL2^{+/+}$ and $CCRL2^{-/-}$ mice. The mice were sacrificed 3 and 6 days later, and the tumors were recovered and digested. The immune cell populations were analyzed by flow cytometry.* ***(A)*** *Total immune cells ($CD45^+$).* ***(B-E)*** *Immune cells subsets amongst $CD45^+$ cells: NK cells ($NK1.1^+$ $CD3^-$), dendritic cells ($CD11c^+$ $CD11b^+$ and $CD11c^+$ $CD11b^-$) and $CD11b^+$ cells (macrophages and MDSC). This data set is representative of 6 independent experiments.*

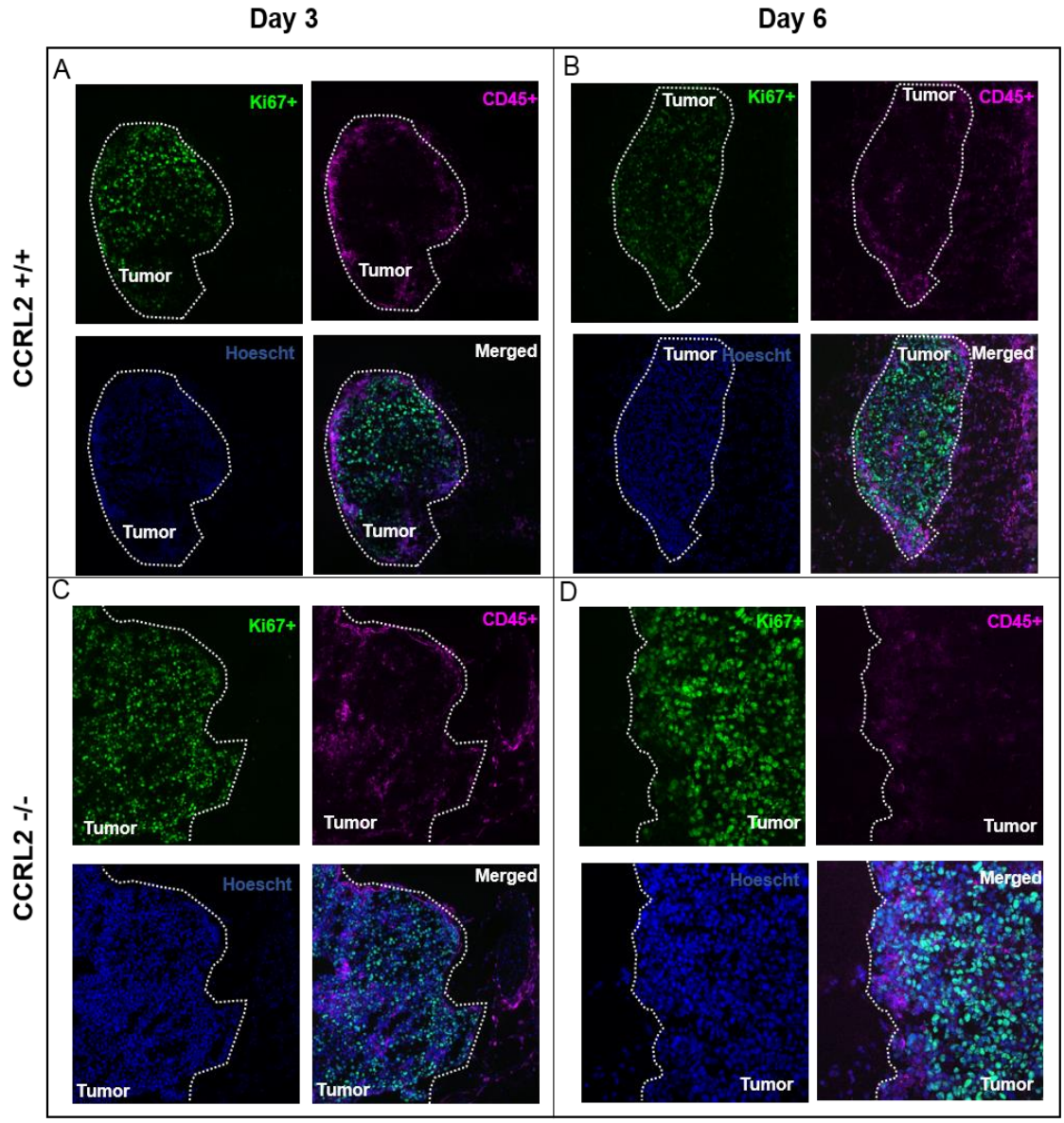

Figure 4.7. CCRL2$^{+/+}$ and CCRL2$^{-/-}$ mice present similar proportion and location of immune cells in tumors. *1.10^{6} B16 cells were injected subcutaneously in the back of CCRL2$^{+/+}$ and CCRL2$^{-/-}$ mice. The mice were sacrificed 3 and 6 days later, the tumors were recovered and embedded, without fixation, in OCT. Immunofluorescente staining was performed on tumor sections from CCRL2$^{+/+}$ and CCRL2$^{-/-}$ mice. Proliferating cells were stained with an anti-Ki67 antibody (green) and immune cells with an anti-CD45 antibody (pink). The nuclei were stained with Hoescht 33342 (blue). Magnification is x10 for panels A, B and C,and x20 for panel D. This data set is representative of 3 independent experiments.*

To confirm that CCRL2 does not affect the immune cell recruitment to tumors, we performed the same experiments on LLC tumors, 10 days after tumor implantation. We injected 1.10^6 LLC cells in $CCRL2^{+/+}$ and $CCRL2^{-/-}$ mice, and sacrificed them ten days after the graft. We removed and digested the tumors and analyzed the immune populations by flow cytometry. We observed that the proportion of $CD45^+$ cells is similar in $CCRL2^{+/+}$ and $CCRL2^{-/-}$ mice (Figure 4.8). The immune cell subsets (T cells, NK cells, dendritic cells and MDSC) were also similar in both groups.

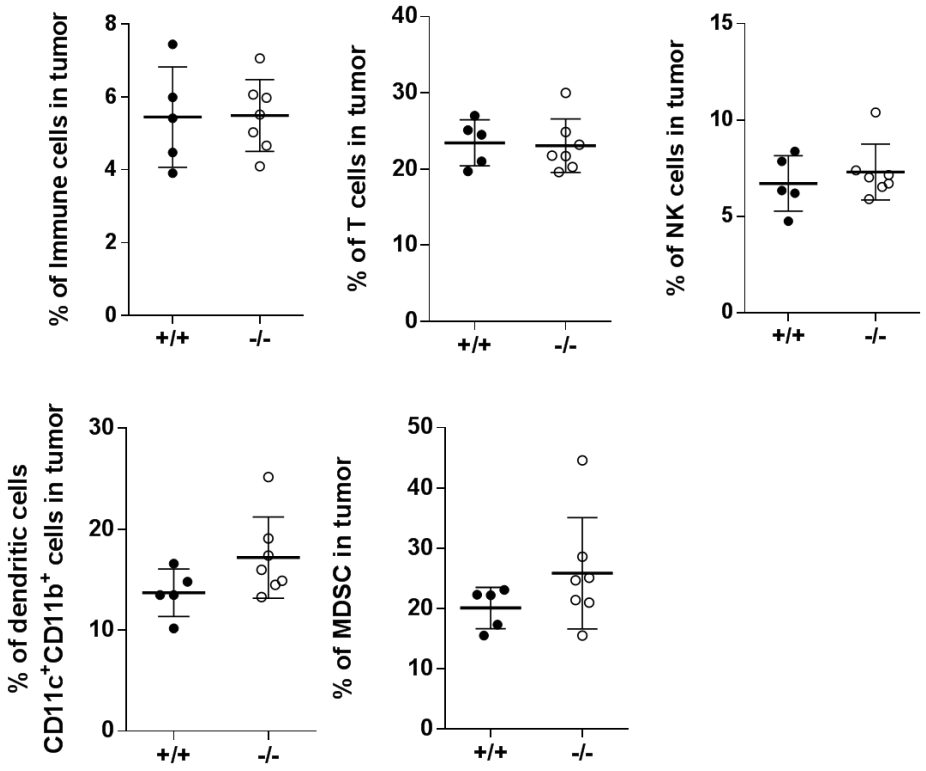

Figure 4.8. The immune cell recruitment is not affected by CCRL2 in LLC tumors. *Flow cytometry of immune cells present in LLC tumors from $CCRL2^{+/+}$ and $CCRL2^{-/-}$ mice. The first graph shows the percentage of total immune cells ($CD45^+$), and the next graphs are representative of immune cells subsets: T cells ($CD3^+$), NK cells ($NK1.1^+$), dendritic cells ($CD11c^+$ $CD11b^+$) and MDSC ($CD11b^+$ $Gr1^+$). This experiment is representative of 3 independent experiments.*

We conclude that the decrease in tumor size observed in CCRL2$^{-/-}$ mice is not dependent on changes in the concentration of chemerin in the blood, neither to the number or proportion of immune cells recruited to the tumor site.

4.5 CCRL2 DOES NOT INFLUENCE THE PROLIFERATION OF TUMOR CELLS, BUT AFFECTS THEIR SURVIVAL

CCRL2 is present on the surface of immune cells, but also on endothelial cells. CCRL2 deficiency might therefore influence tumoral neoangiogenesis and as a consequence tumor cell survival and proliferation rate. We analyzed the proliferation and apoptosis of tumor cells by detecting specific markers by immunofluorescence. To analyze the tumor proliferation at early stages following grafting, we collected tumors from wild-type and CCRL2 knock-out mice at day 3 and day 6 of tumor development. Cryosections of tumors were performed and the proliferation of tumor cells was determined by staining with an anti-Ki67 antibody. To quantify the proportion of proliferating cells, we analyzed the colocalization between Ki67 staining and Hoechst staining (Figure 4.9). No difference was observed between CCRL2$^{+/+}$ and CCRL2$^{-/-}$ mice at day 3 and day 6 of tumor development.

These results suggest that CCRL2 does not affect the proliferation of tumor cells. Proliferation of tumor cells increases the requirement for oxygen and nutrients provided by the vascularization. To identify apoptotic cells in tumors, CCRL2$^{+/+}$ and CCRL2$^{-/-}$ mice were injected with 1.10^6 LLC. Ten days after tumor implantation, tumors were removed and we performed hematoxylin/eosin staining and immunofluorescence analyses of apoptotic and endothelial cells (Figure 4.10).

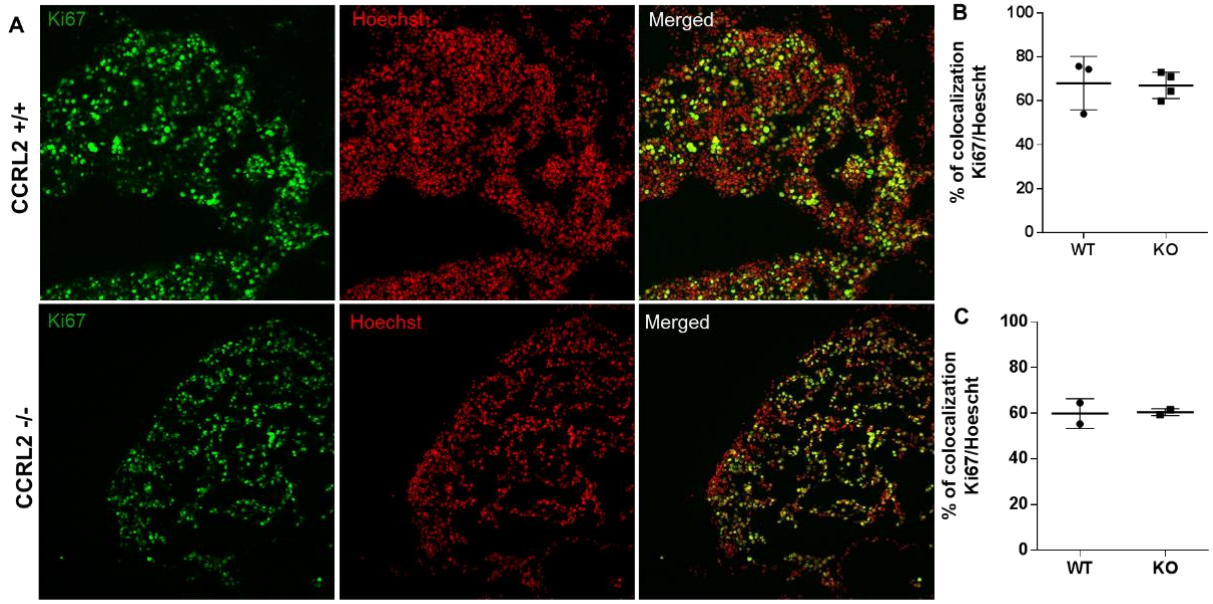

Figure 4.9. B16 tumors from CCRL2$^{+/+}$ and CCRL2$^{-/-}$ mice display a similar proportion of proliferating cells. *1.10^6 B16 cells were injected subcutaneously in the back of CCRL2$^{+/+}$ and CCRL2$^{-/-}$ mice. The mice were sacrificed at 3 and 6 days, the tumors were recovered and embedded, without fixation, in OCT, and immunofluorescence staining was performed on tumor section.* ***A.*** *Proliferating cells were stained with an anti-Ki67 antibody (green) and the nuclei were stained with Hoechst 33342 (blue). Only tumors collected on day 6 are illustrated. Magnification 10x.* ***B, C.*** *Percentage of proliferating cells (Ki67$^+$ Hoescht 33342$^+$ cells) in tumors from CCRL2$^{+/+}$ and CCRL2$^{-/-}$ mice at day 3 (B) and day 6 (C). The percentage of colocalization is calculated with the Jacop plugin of Image J software. This experiment was performed only once.*

Apoptotic cells and endothelial cells were identified by anti-cleaved caspase 3 and anti-CD31 antibodies respectively. We observed a significant increase in the surface of necrotic areas and in the number of apoptotic cells at the periphery of these necrotic areas in tumors from CCRL2$^{-/-}$ mice. The staining by the anti-cleaved caspase 3 antibody was indeed much more widespread as compared to CCRL2$^{+/+}$ mice. These data seem to indicate that CCRL2 could affect the apoptosis and necrosis processes in the LLC tumor model. We could however not

conclude so far regarding potential differences in the number of blood vessels detected by the CD31 antibody.

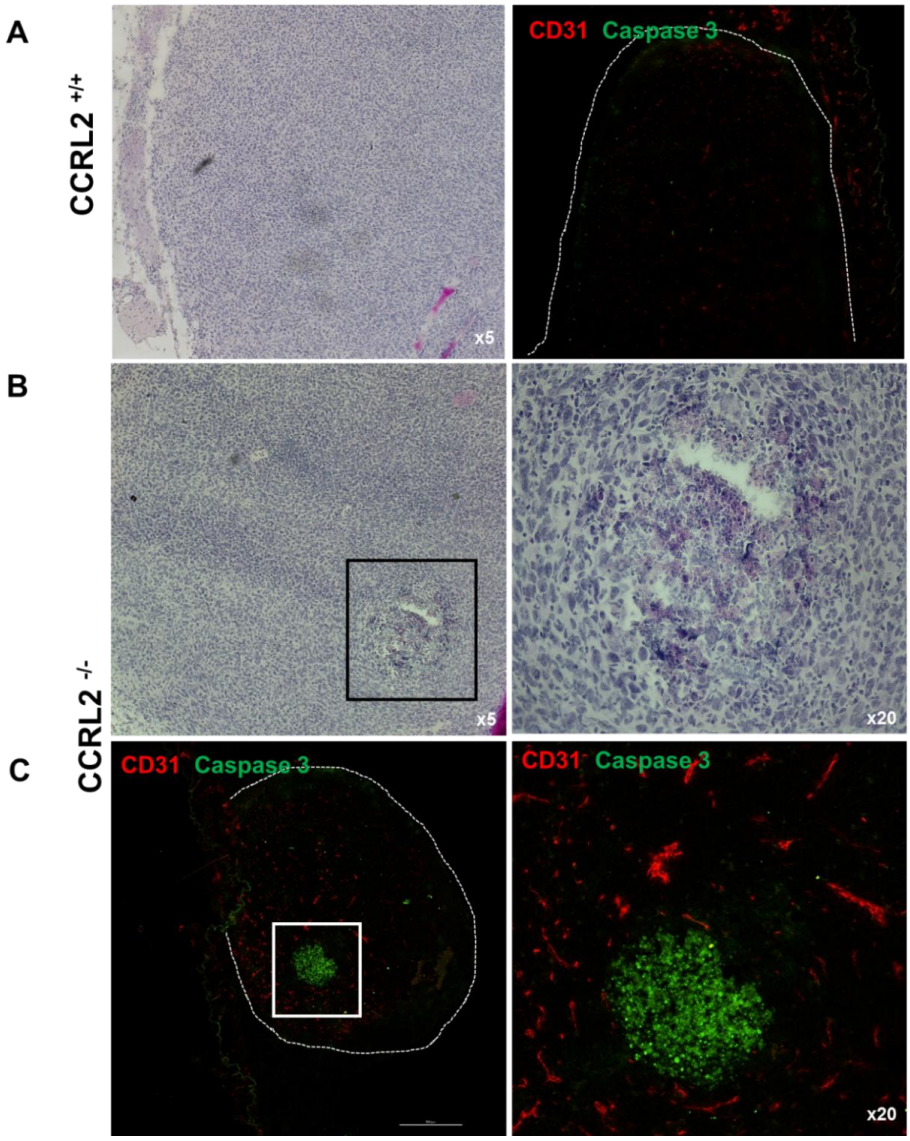

Figure 4.10. In the absence of CCRL2, tumors present an increase in necrotic areas and apoptotic cells. *LLC cells were injected subcutaneously in the back of CCRL2$^{+/+}$ and CCRL2$^{-/-}$ mice. The mice were sacrificed 10 days later, and the tumors were removed and embedded, without fixation, in OCT.* ***A.*** *Representative views of HE staining (left panel) and CD31 and active caspase 3 immunostaining (right panel) for one of the 5 tumors from wild-type mice.* ***B and C****. Representative HE staining (B) and CD31 and active caspase 3 immunostaining (C) of one of the 5 tumors from CCRL2 knock-out mice. The tumors were stained with an anti CD31 antibidy coupled to PE and an anti-cleaved caspase 3 antibody detected by a secondary antibody coupled to FITC. Endothelial cells are therefore stained in red and apoptotic cells in green. Magnification x5 and x20 as indicated on the panels. These data are representative of 2 independent experiments.*

4.6 THE EXPRESSION OF ANGIOGENIC AND INFLAMMATORY FACTORS IS MODIFIED IN CCRL2-DEFICIENT MICE

Apoptotic and necrotic processes are closely linked to the tumor microvascularization. Indeed, the angiogenesis allows to support the supply of oxygen and nutrients necessary to tumor development. CCRL2 is expressed by endothelial cells, suggesting that this receptor might be important for the function of these cells and more precisely tumor neoangiogenesis (Gonzalvo-Feo et al., 2014). Endothelial cells proliferate and migrate to the tumor site in response to the secretion of angiogenic factors by tumor cells, pro-tumoral immune cells or cells from the tumor microenvironment. To determine whether CCRL2 deficiency affects the neoangiogenic process supporting tumor survival and growth, we quantified the expression of several angiogenic and inflammatory factors in LLC tumors from $CCRL2^{+/+}$ and $CCRL2^{-/-}$ mice. 1.10^6 LLC cells were injected in the flank mice, and the tumors were recovered ten days later. We extracted the RNA from the tumors, and by qPCR, analyzed the expression of angiogenic and inflammatory factors, including TSP1, TNFα, TGFβ, IFNγ, VEGFA, FGF2, MMP9, MMP10, CCL2, CXCL1, CXCL2, IL1β, IL-6 and IL-10. We observed that, in the absence of CCRL2, the expression of TSP1, VEGFA and FGF2 was increased as compared to control mice (Figure 4.11). Others factors were altered in the absence of CCRL2, such as MMP9, TNFα and IL-6, but these results were not confirmed in a second experiment and it will be necessary to perform additional repeats of this protocol a different time points of tumor development, in order to concluded regarding the whole set of markers that was tested so far. These preliminary data suggest however that CCRL2 might have a significant influence on the control of tumoral angiogenesis, by modulating the expression of angiogenic factors.

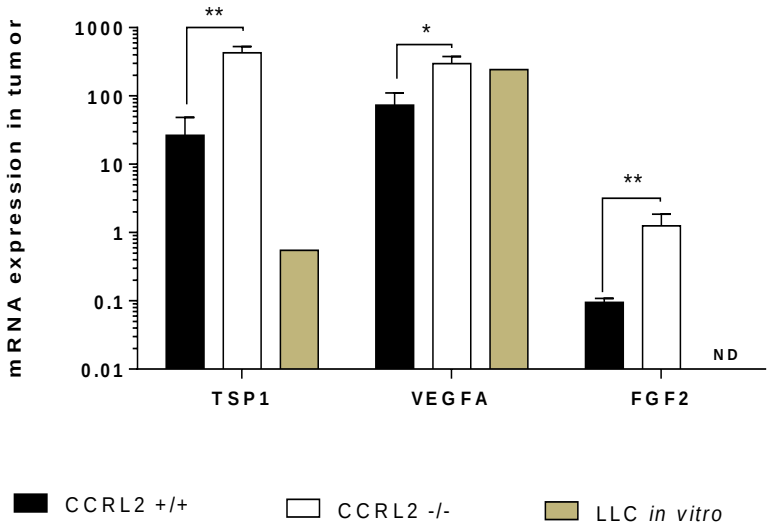

Figure 4.11 CCRL2 invalidation affects the expression of thrombospondin-1, VEGFA and FGF2 in LLC tumors. LLC t*umors from CCRL2$^{+/+}$ and CCLR2$^{-/-}$ mice, at day 10 of development, were recovered and digested. RNA was extracted, and qPCR was performed. The gene expression levels are relative to thje reference housekeeping gene GAPDH. This data set is representative of 2 independent experiments. * and ** represent p values of < 0.05 and < 0.01 respectively, ND = not detected.*

5. DISCUSSION

Several studies showed a correlation between the chemerin concentration in plasma or chemerin expression by tumors and the prognosis of human cancers, suggesting a role of chemerin in the physiopathology of cancer (Wang et al., 2014) (Pachynski et al, 2012). Our work has as main objective to understand the role of chemerin receptors in tumor development. First, we want to determine which receptor is involved in the control of tumor initiation and progression. To answer this question, we used genetically invalidated mice for each receptor and wild-type mice as controls, and these mice were injected with two syngeneic tumor cell lines, the B16 melanoma and Lewis lung carcinoma lines.

It is known that ChemR23, the main chemerin receptor, is implicated in the migration of immune cells in response to chemerin, and the chemerin-ChemR23 system is involved in various inflammatory diseases (Luangsay et al., 2009). Our results show however that ChemR23 does not affect tumor growth in our experimental models, neither the immune cell recruitment to the tumor site. ChemR23 does not seem therefore to play a significant role in the growth of established tumor cells. It remains possible however that ChemR23 is involved in the early steps of tumor initiation, such as in the chronic inflammatory processes that predispose to tumor development.

CCRL2 is described as a non-functional receptor, because chemerin binding does not result in the activation of signaling cascades nor in receptor internalization. A recent study showed that this receptor allows dendritic cell migration to lymph nodes in a model of ovalbumin-induced airway inflammation (Otero et al., 2010). It was also proposed that CCRL2 acts by concentrating chemerin at the cell surface and presenting the ligand to ChemR23-expressing cells (Zabel et al., 2008).

When we analyzed the growth of tumoral cell lines in CCRL2-deficient mice, we observed a reduction of tumor size, as compared to wild-type mice, suggesting a

pro-tumoral effect of CCRL2. This effect cannot be explained by a default of immune recruitment neither by an alteration of plasmatic chemerin levels. These results suggest that the role of CCRL2 is not related to changes in the efficiency of immune cell recruitment to the tumor in response to chemerin.

In order to further test the relative roles of CCRL2 and ChemR23 in a tumor context, we suggest the generation of mice deficient for both ChemR23 and CCRL2. It is indeed still possible that the absence of CCRL2 modifies the local concentrations or the presentation of bioactive chemerin without affecting the circulating levels, and that the final outcome on tumor growth does involve ChemR23. Testing tumor growth and immune cell recruitment in mice invalidated for both receptors would allow to test this hypothesis. If deficient mice for the two receptors develop tumors similarly to CCRL2-deficient mice, it would confirm that ChemR23 is not involved in the phenotype of these mice.

Tumor microenvironment is critical for the survival of tumor cells. Neovascularization of tumor enables tumor cell proliferation by supporting the supply of oxygen and nutrients, thereby avoiding apoptosis and necrosis of tumor cells. CCRL2 is known to be expressed by endothelial cells. Thus, we were interested to understand the potential role of CCRL2 on tumor cell proliferation and survival and the neoangiogenesis process. Our results show that the proliferation of tumor cells is not affected by the absence of CCRL2, suggesting that CCRL2 is not fundamental to the direct control of tumor growth. In CCRL2-deficient mice, an increase in the number of apoptotic cells and in the size of necrotic regions was however observed in the tumors, suggesting that CCRL2 affects tumor cell survival. Increase cell death by apoptosis and necrosis can be the result of insufficient oxygen supply, resulting from a relative defect in angiogenesis. We stained endothelial cells in tumor sections by using anti-CD31 antibodies, but could not detect significant differences in the density of blood vessels. However, the size of the tumors was quite different between CCRL2-invalidated mice and their controls, and the interpretation of blood vessel density is therefore difficult. To

better understand the cause of apoptotic and necrotic processes in CCRL2 KO mice, we suggest the staining of hypoxic regions in tumors with pimonidazole. This marker is able to bind to thiol-containing proteins when the oxygen concentration in the microenvironment is low.

In order to understand if increased apoptosis in the absence of CCRL2 may be the result of poor vascularization, we observed the expression of several angiogenic factors in tumors. The results show an increase of TSP-1, VEGFA and FGF2 transcripts in the absence of CCRL2. Thrombospondin-1 is a matrix glycoprotein expressed by endothelial cells, adipocytes, smooth muscle cells, fibroblasts, monocytes and macrophages. It regulates the structure of the extracellular matrix, extracellular proteases and levels of active TGF-β, resulting in an inhibition of tumor growth (Lawler, 2002) (Lopez-Dee et al., 2011). TSP1 is considered as a regulator of angiogenesis with direct and indirect effects. TSP1 affects angiogenesis indirectly by activation of TGF-β, which induces the apoptosis of endothelial cells. TSP1 can also directly inhibit the migration of endothelial cells and induce their apoptosis, through interaction with its receptor CD36. This interaction can inhibit survival pathways promoted by VEGF and FGF2 (Lawler, 2002).

Knowing that CCRL2 and TSP1 are both expressed by endothelial cells, we propose the hypothesis that CCRL2 would negatively regulate the expression of TSP1. To test this hypothesis, it will be necessary to test the expression of TSP1 at different time points during tumor development and in control conditions.

The increased expression of VEGFA and FGF2 in the absence of CCRL2 could be explained by different mechanisms. The two genes might be downregulated directly or indirectly by CCRL2, but the increased expression of VEGFA and FGF2 in tumors of CCRL2$^{-/-}$ mice is not really compatible with inefficient angiogenesis leading to tumor cell apoptosis and necrosis. Alternatively, this increased expression might rather be the consequence of hypoxia, and therefore secondary

to the increased expression of TSP1 and the angiogenesis defect in CCRL2$^{-/-}$ mice. This is the hypothesis we favor at present. To prove this hypothesis, it will be important to analyze the relative expression of the three angiogenesis regulators all along the development of tumors in order to determine which factor is modified first. It would also be interesting to test the expression of the receptors of VEGFA (VEGFR1 and VEGFR2) and FGF2 (FGFR1 and FGFR2) to test whether the increase in the two growth factors might be inefficient as a result of receptor downmodulation.

The migration of endothelial cells can be a result of three different processes: chemotaxis, haptotaxis or mechanotaxis. The chemotaxis consists in the directional migration in response to a gradient of soluble chemoattractants. The main factors involved in chemotaxis of endothelial cells are VEGF, bFGF and angiopoietins, and the minor factors are FGF2, TGF-β, interleukins and TNF-α (Lamalice et al., 2007). We propose the hypothesis that CCRL2 can influence the chemotaxis of endothelial cells. If CCRL2 is absent, the endothelial cells might migrate less efficiently to the center of the tumor, in response to VEFGA and FGF2. As a result of defective angiogenesis, the local concentration of these two growth factors would increase further, while necrosis and apoptosis would be favored in the tumor. To understand further the potential defect in tumor angiogenesis in the absence of CCRL2, we suggest to complement the CD31 labeling we performed by the immunofluorescence staining of blood vessels with a lectin coupled to FITC. Intraperitoneal injection of lectin-FITC in mice allows visualizing the tumor microvasculature with great details by fluorescence microscopy on tumors collected an hour later.

It will also be important to test the role of CCRL2 in non tumoral angiogenesis. For this purpose, we propose to investigate the angiogenic response to VEGF in a model such as the mouse cornea micropocket angiogenesis assay, or similar assays that are perfomed in the back skin of mice, and compare CCRL2$^{-/-}$ and wild-type mice.

6. CONCLUSION

In this work, we have shown that ChemR23, the major chemerin receptor, does not affect the tumor growth or the leukocyte recruitment, suggesting that this receptor is not implicated in the antitumoral effects of chemerin observed in the B16 and LLC tumor models. In contrast, CCRL2, a non-functional chemerin receptor, display a pro-tumoral effect in the same experimental models. This effect is presumably due to the fact that CCRL2 appears as a positive regulator of angiogenesis, with a potential implication of thrombospondin 1, or implicated in the migration of endothelial cells. As a result of improved supply of oxygen and nutrients, CCRL2 would protect tumor cells from necrosis and apoptosis.

7. Bibliography

- Macheret, M., & Halazonetis, T. D. (2015). **DNA replication stress as a hallmark of cancer**. Annual Review of Pathology, *10*, 425–48. 158
- Direção-Geral de Saude. **Portugal: Doenças Oncológicas em números – 2014**. Novembro, 2014
- **World cancer factsheet**. (2014), *2012*(2012), 2012–2015.
- Broertjes J. (2015). **The ten hallmarks of Cancer in Cutaneous Malignant Melanoma. UNAV Journal fo Medical Students.** Volume 1, June 2015, p.6.
- Herceg, Z. (2007). **Epigenetics and cancer : towards an evaluation of the impact of environmental and dietary factors**, *22*(2), 91–103. doi:10.1093/mutage/gel068
- Boffetta, P., & Nyberg, F. (2003). **Contribution of environmental factors to cancer risk**, *68*, 71–94. doi:10.1093/bmb/ldg023
- Brennan, P. (2002). **Gene – environment interaction and aetiology of cancer : what does it mean and how can we measure it ?,** *23*(3), 381–387.
- Hanahan, D., & Weinberg, R. a. (2011). **Hallmarks of cancer: the next generation**. *Cell*, *144*(5), 646–74. doi:10.1016/j.cell.2011.02.013
- Horta, T., Butera, A. P., Henriques, D., Leal, S., & Alves, R. J. (2007). **Agentes antitumorais inibidores da angiogenese - Modelos farmacofóricos para inibidores da integrina αvβ** 3, *43*, 1–17.
- Horssen, R. Van, Hagen, T. L. M., & Eggermont, A. M. M. (2006). **Sarcomas TNF- α in Cancer Treatment : Molecular Insights , Antitumor Effects , and Clinical Utility**. The Oncologyst, 397–408.
- Stockmann, C., Schadendorf, D., Klose, R., & Helfrich, I. (2014**). The impact of the immune system on tumor: angiogenesis and vascular remodeling**. *Frontiers in Oncology*, *4*(April), 69. doi:10.3389/fonc.2014.00069
- Finn, O. J. (2012**). Immuno-oncology: understanding the function and dysfunction of the immune system in cancer**. *Annals of Oncology : Official*

Journal of the European Society for Medical Oncology / ESMO, *23 Suppl 8*(Supplement 8), viii6–9. doi:10.1093/annonc/mds256

- Chimal-Ramírez, G. K., Espinoza-Sánchez, N. A., Fuentes-Pananá, E. M. (2013). **Protumor Activities of the Immune Response : Insights in the Mechanisms of Immunological Shift , Oncotraining , and Oncopromotion**. Journal of Oncology, ID 835956, *2013*.
- Quail, DF., Joyce, JA. (2013). **Microenvironmental regulation of tumor progression and metastasis**. Nat Med, November 2013. NIH Public Access, *19*(11), 1423–1437. doi:10.1038/nm.3394.
- Gallimore, A. M., & Simon, A. K. (2008). **Positive and negative influences of regulatory T cells on tumour immunity.** Oncogene. 5886–5893. doi:10.1038/onc.2008.269
- Watanabe, S., Deguchi, K., Zheng, R., Tamai, H., Wang, L. -x., Cohen, P. a., & Shu, S. (2008). **Tumor-Induced CD11b+Gr-1+ Myeloid Cells Suppress T Cell Sensitization in Tumor-Draining Lymph Nodes**. *The Journal of Immunology*, *181*(5), 3291–3300. doi:10.4049/jimmunol.181.5.3291
- Liu, C., Yu, S., Kappes, J., Wang, J., Grizzle, W. E., Zinn, K. R., & Zhang, H. (2007). **Expansion of spleen myeloid suppressor cells represses NK cell cytotoxicity in tumor-bearing host.** Blood Journal, May 2007. *109*(10), 4336–4343. doi:10.1182/blood-2006-09-046201.The
- Allavena, P., Germano, G., Marchesi, F., & Mantovani, A. (2011). **Chemokines in cancer related inflammation.** *Experimental Cell Research*, *317*(5), 664–73. doi:10.1016/j.yexcr.2010.11.013
- Zhao, X., Jain, S., Benjamin Larman, H., Gonzalez, S., & Irvine, D. J. (2005). **Directed cell migration via chemoattractants released from degradable microspheres**. *Biomaterials*, *26*(24), 5048–63. doi:10.1016/j.biomaterials.2004.12.003
- Pachynski, R. K., Zabel, B. a, Kohrt, H. E., Tejeda, N. M., Monnier, J., Swanson, C. D. Butcher, E. C. (2012). **The chemoattractant chemerin**

suppresses melanoma by recruiting natural killer cell antitumor defenses. *The Journal of Experimental Medicine*, *209*(8), 1427–35. doi:10.1084/jem.20112124

- Wang, C., Wu, W. K. K., Liu, X., To, K.-F., Chen, G. G., Yu, J., & Ng, E. K. W. (2014**). Increased serum chemerin level promotes cellular invasiveness in gastric cancer: a clinical and experimental study.** *Peptides*, *51*, 131–8. doi:10.1016/j.peptides.2013.10.009
- Zabel, B. A., Kwitniewski, M., Banas, M., Zabieglo, K., & Murzyn, K. (2014). **Chemerin regulation and role in host defense**. Journal Clinical Experimenta Immunology, March 2014. *3*(1), 1–19.
- Mattern, A., Zellmann, T., & Beck-Sickinger, A. G. (2014**). Processing, signaling, and physiological function of chemerin**. *IUBMB Life*, *66*(1), 19–26. doi:10.1002/iub.1242
- Du, X., & Leung, L. L. K. (2009). **Proteolytic regulatory mechanism of chemerin bioactivity**. Acta Biochim Biophys Sin, 2009, Volume 41, Issue 12, Page 973-979.
- Wittamer, V., Franssen, J.-D., Vulcano, M., Mirjolet, J.-F., Le Poul, E., Migeotte, I., Communi, D. (2003). **Specific recruitment of antigen-presenting cells by chemerin, a novel processed ligand from human inflammatory fluids**. *The Journal of Experimental Medicine*, *198*(7), 977–85. doi:10.1084/jem.20030382
- Arita, M., Ohira, T., Sun, Y.-P., Elangovan, S., Chiang, N., & Serhan, C. N. (2007). **Resolvin E1 Selectively Interacts with Leukotriene B4 Receptor BLT1 and ChemR23 to Regulate Inflammation**. *The Journal of Immunology*, *178*(6), 3912–3917. doi:10.4049/jimmunol.178.6.3912
- Bondue, B., Wittamer, V., & Parmentier, M. (2011). **Chemerin and its receptors in leukocyte trafficking, inflammation and metabolism.** *Cytokine & Growth Factor Reviews*, *22*(5-6), 331–8. doi:10.1016/j.cytogfr.2011.11.004

- Wu, J., Xie, N. A., Zhao, X. I. A., Nice, E. C., & Huang, C. (2012). **Dissection of Aberrant GPCR Signaling in Tumorigenesis – A Systems Biology Approach**,. Cancer Genomics & Proteomics 9, 37–50.
- Tuteja, N. (2009). **Signaling through G protein coupled receptors,**. Plant signaling & Behavior, Volume *4* (10), 942–947.
- Herová, M., Schmid, M., Gemperle, C., & Hersberger, M. (2015). **ChemR23, the receptor for chemerin and resolvin E1, is expressed and functional on M1 but not on M2 macrophages.** *Journal of Immunology (Baltimore, Md. : 1950)*, *194*(5), 2330–7. doi:10.4049/jimmunol.1402166
- Luangsay, S., Wittamer, V., Bondue, B., De Henau, O., Rouger, L., Brait, M., … Parmentier, M. (2009). **Mouse ChemR23 is expressed in dendritic cell subsets and macrophages, and mediates an anti-inflammatory activity of chemerin in a lung disease model.** *Journal of Immunology (Baltimore, Md. : 1950)*, *183*(10), 6489–99. doi:10.4049/jimmunol.0901037
- Zabel, B. a, Nakae, S., Zúñiga, L., Kim, J.-Y., Ohyama, T., Alt, C., … Butcher, E. C. (2008**). Mast cell-expressed orphan receptor CCRL2 binds chemerin and is required for optimal induction of IgE-mediated passive cutaneous anaphylaxis**. *The Journal of Experimental Medicine*, *205*(10), 2207–20. doi:10.1084/jem.20080300
- Gonzalvo-Feo, S., Del Prete, A., Pruenster, M., Salvi, V., Wang, L., Sironi, M. … Sozzani, S. (2014). **Endothelial cell-derived chemerin promotes dendritic cell transmigration**. *Journal of Immunology (Baltimore, Md. : 1950)*, *192*(5), 2366–73. doi:10.4049/jimmunol.1302028
- Mekada, K., Abe, K., Murakami, A., Nakamura, S., Nakata, H., Moriwaki, K., Yoshiki, A. (2009). **Genetic Differences among C57BL / 6 Substrains**, *58*(December 2008), 141–149.
- Bobek, V., Kolostova, K., Pinterova, D., Kacprzak, G., Adamiak, J., & Kolodziej, J. (2010**). A Clinically Relevant , Syngeneic Model of Spontaneous , Highly Metastatic B16 Mouse Melanoma**, *4804*, 4799–4803.

- Kellar, A., Egan, C., & Morris, D. (2015). **Preclinical Murine Models for Lung Cancer : Clinical Trial Applications**, *2015*.
- Jahan-Tigh, R. R., Ryan, C., Obermoser, G., & Schwarzenberger, K. (2012). **Flow cytometry**. *The Journal of Investigative Dermatology*, *132*(10), e1. doi:10.1038/jid.2012.282
- Odell, I. D., & Cook, D. (2013). **Immunofluorescence techniques**. *The Journal of Investigative Dermatology*, *133*(1), e4. doi:10.1038/jid.2012.455
- Nwaneshiudu, A., Kuschal, C., Sakamoto, F. H., Anderson, R. R., Schwarzenberger, K., & Young, R. C. (2012). **Introduction to confocal microscopy**. *The Journal of Investigative Dermatology*, *132*(12), e3. doi:10.1038/jid.2012.429
- Fisher, A. H.; Jacobson, K. A.; Rose, J.; Zeller, R.. Adapted from "**Preparation of Cells and Tissues for Fluorescence Microscopy**," Chapter 4, in Basic Methods in Microscopy (eds. Spector and Goldman). Cold Spring Harbor Laboratory Press, Cold Spring Harbor, NY, USA, 2006.
- Gan, S. D., Patel, K. R., & Elisa, S. (2013). **Enzyme Immunoassay and Enzyme-Linked Immunosorbent Assay,** *133*(9), e12–3. doi:10.1038/jid.2013.287
- Gentle A., Anastasopoulos F., McBrien N. A., (2001). **High-Resolution Semi Quantitative Real-Time PCR without the Use of a Standard Curve.** *BioTechniques,* September 2001. Doi: 31:502-508
- Ho-Pun-Cheung, A., Bascoul-Mollevi, C., Assenat, E., Boissière-Michot, F., Bibeau, F., Cellier, D., Lopez-Crapez, E. (2009). **Reverse transcription-quantitative polymerase chain reaction: description of a RIN-based algorithm for accurate data normalization**. *BMC Molecular Biology*, *10*(1), 31. doi:10.1186/1471-2199-10-31
- Santos, C. F.; Sakai, V. T.; Machado, M. A.; Schippers, D. N.; Greene,, A. S.. (2004) **Reverse transcription and polymerase chain reaction: principles and applications in dentistry**. J Appl Oral Science, 2004; 12(1):1-11.

- Kupiec, T. (2004). **Quality-Control Analytical Methods : High-Performance Liquid Chromatography**, *8*(3), 223–227.
- Xiong S., Zhang L., He QY, (2008). Fractionation of proteins by heparin chromatography. Methods Molecular Biology, 2008. doi: 10.1007/978-1-60327-064-9_18.
- Oksa V. V., Kivela P. (2009). **Aequorin bioluminescence assays on MicroBeta2 LumiJET for studying Ca2+-coupled GPCRs and ion channels**. Perkinelmer, 008448_01
- Rank, M., Sig, E., & Sig, E. (1988). 7.2. **Teste de wilcoxon-mann-whitney**, 219–232.
- *Graham Hole Research Skills, version 1.0 (n. d.).* **The Wilcoxon test.**
- Otero, K., Vecchi, A., Hirsch, E., Kearley, J., Vermi, W., Del Prete, A., Sozzani, S. (2010). **Nonredundant role of CCRL2 in lung dendritic cell trafficking**. *Blood*, *116*(16), 2942–9. doi:10.1182/blood-2009-12-259903
- Vermi, W., Riboldi, E., Wittamer, V., Gentili, F., Luini, W., Marrelli, S., Sozzani, S. (2005). **Role of ChemR23 in directing the migration of myeloid and plasmacytoid dendritic cells to lymphoid organs and inflamed skin**. *The Journal of Experimental Medicine*, *201*(4), 509–15. doi:10.1084/jem.20041310
- Yoshimura, T., & Oppenheim, J. J. (2010). Chemokine-like receptor 1 (CMKLR1) and chemokine (C-C motif) receptor-like 2 (CCRL2); two multifunctional receptors with unusual properties. *Experimental Cell Research*, *317*(5), 674–84. doi:10.1016/j.yexcr.2010.10.023
- Lawler, J. (2002). Thrombospondin-1 as an endogenous inhibitor of angiogenesis and tumor growth. Journal Cell Mol. Med. Vol *6*(1), 1–12.
- Lopez-Dee, Z., Pidcock, K., & Gutierrez, L. S. (2011). Thrombospondin-1: Multiple Paths to Inflammation. *Mediators of Inflammation*, *2011*, 1–10. doi:10.1155/2011/296069

- Lamalice, L., Le Boeuf, F., & Huot, J. (2007). Endothelial cell migration during angiogenesis. *Circulation Research*, *100*(6), 782–94. doi:10.1161/01.RES.0000259593.07661.1e